Journal of Analytical and Applied Pyrolysis 169 (2023) 105864

Contents lists available at ScienceDirect

Journal of Analytical and Applied Pyrolysis

journal homepage: www.elsevier.com/locate/jaap

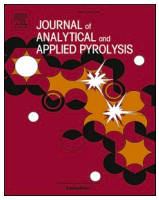

# Employment of conventional and flash pyrolysis for biomass wastes from the textile industry with sustainable prospects

Begoña Ruiz [a], Enrique Fuente [a], Alejandro Pérez [a], Luis Taboada-Ruiz [a], Juan Marcos Sanz [b], Luis Fernando Calvo [c], Sergio Paniagua [d,e,*]

[a] Biocarbon, Circularity and Sustainability Group (BC&S), Instituto de Ciencia y Tecnología del Carbono (INCAR), CSIC, Francisco Pintado Fe, 26, 33011 Oviedo, Spain
[b] Textil Santanderina, S.A., R+D Department, Avenida Textil Santanderina s/n, Cabezón de la Sal 39500, Spain
[c] University of León, Department of Chemistry and Applied Physics, Chemical Engineering Area, IMARENABIO, Avda. Portugal 41, 24071 León, Spain
[d] University of Valladolid, Department of Applied Physics, 47011 Valladolid, Spain
[e] Institute of Sustainable Processes, University of Valladolid, Valladolid 47011, Spain

ARTICLE INFO

*Keywords:*
Card waste
Short fibre waste
Wool
Flash pyrolysis
Bio-char
Bio-fuel

ABSTRACT

The textile industry generates millions of tons of waste annually, making this sector one of the most polluting in the world. The objective of this research was to study the energy potential of three industrial textile wastes of vegetable and animal origin: CW (card waste), SFW (short fibre waste) and W (wool), using conventional and flash pyrolysis at 500 °C and 750 °C. CW and SFW thermogravimetric profiles were very different from W. In general, the bio-oil yield was higher in the conventional and in the low-temperature flash pyrolysis (up to 55 %). The gas obtained by flash pyrolysis at 750 °C has higher flue gas content and lower $CO_2$ content so their high heating value (HHV) is higher (up to 15.34 MJ/kg). Bio-oils obtained by flash pyrolysis at high temperature stood out for their higher HHV (>30 MJ/kg), with the highest value (34.15 MJ/kg) obtained from SFW waste. Both low temperature flash pyrolysis and conventional pyrolysis produce bio-oils that contain aromatic (35–48 %) and non-aromatic (18–34 %) organic compounds. Additionally, they have high levels of phenols and benzenes. High-temperature flash pyrolysis bio-oils are mainly composed of polycyclic aromatic hydrocarbons. The textile samples are suitable for an energetic valorisation, highlighting the best SWF behaviour.

## 1. Introduction

Millions of tons of textile waste are produced each year. Therefore, ensuring its proper management is one of the current global challenges [1]. The textile industry produces a significant amount of organic solid waste that has a huge impact on environmental pollution [2]. With 3 % of all greenhouse gas emissions (GHG), this industry has risen to the top of the list of those that pollute the planet [3]. The textile sector releases a lot of pollutants into the environment, including liquid discharge, solid waste, and gases [4].

Based on its status and quality, textile waste can be divided into reusable and non-reusable waste. Unfortunately, despite the enormous efforts that numerous researchers and organizations are making [5], recycling or utilisation of solid organic textile wastes as raw material for manufacture to useful products is not being a widely used alternative so far today [6]. More than 69 % of this waste is landfilled [7]. This fact encompass many environmental concerns such as GHG emissions, soil contamination and production of toxic leachates and biogases [8].

These factors make the usual means of textile waste disposal less acceptable in terms of secondary environmental degradation [9]. When the cost of reuse or recycling exceeded its economical values, waste energy recovery was encouraged [10]. Therefore, rather than disposal, the use of textile wastes for energy conversion will be advantageous in terms of natural resource consumption [11].

When compared to fuel-oil, wood pellets, and wood chips, textile waste is thought to offer a fuel price reduction of between 70 % and 80 % [12]. A common method of disposing of textile waste is thermal treatment, which enables energy recovery and the creation of chemical and

*Abbreviations:* **CW**, Card Waste; **EDX**, Energy-dispersive X-ray; **F**, Flash pyrolysis; **FC**, Fixed Carbon; **HHV**, Higher heating value; **LHV**, Lower heating value; **P**, Conventional pyrolysis; **SEM**, Scanning electron microscope; **SFW**, Short Fibre Waste; **TCD**, Thermal conductivity detector; **TGA**, Thermogravimetric analysis; **VM**, Volatile matter; **W**, Wool.

* Corresponding author at: University of Valladolid, Department of Applied Physics, 47011 Valladolid, Spain.
*E-mail address:* sergio.paniagua@uva.es (S. Paniagua).

https://doi.org/10.1016/j.jaap.2023.105864
Received 23 October 2022; Received in revised form 30 December 2022; Accepted 10 January 2023
Available online 11 January 2023

oil products [13]. However, the raw waste also has the inherent disadvantages of low calorific value and high oxygen contents, causing it unsuitable for direct combustion [14]. Pyrolysis is used as a desirable substitute for incineration to maximize the financial gains from the treatment of textile waste. This thermal process is based on direct thermal decomposition of the organic matter in an inert atmosphere to obtain a wide range of fuels, solvents, chemicals and other products from biomass feedstock [15]. Pyrolysis products such as various liquids (i.e., bio-oils and tars) and gases can be directly used as fuel owing to their higher heating value (HHV) or be converted to several useful chemicals [16]. The pyrolysis process, based on the heating rate, can be classified, among others, into: conventional, fast and flash pyrolysis. Conventional pyrolysis, is the heating of the biomass/organic material in the absence or with a limited supply of oxygen with a slow heating rate, low temperature (<600 °C) and produces a solid product, called bio-char or simply char, bio-oil and gas. Fast and flash pyrolysis occurs at higher heating rate and with considerably shorter annealing time (much shorter in flash pyrolysis) than conventional pyrolysis, and both methods favour the yield of bio-oil and gases over char [17].

The cellulose content of a raw material has a significant impact on how much energy is recovered; cellulose is particularly prevalent in textile waste (40–60 wt%) [18]. Therefore, this thermal process is recommended for these residues [19]. This thermal process encompasses an air-free thermal decomposition of organics with produces a combination of gases, liquids, and/or solid products. In term of pyrolysis products, gases were generated by the cracking of specific functional groups. Chen et al. [20] have demonstrated that the hemicellulose had the highest $CO_2$ yield, whereas lignin had the highest $CH_4$ yield due to the aromatic rings and methoxy groups in lignin structure. Whereas cellulose demonstrated the highest CO yield at high temperatures (above 550 °C).

Both the selection of feedstock and the pyrolysis-type are critical points to consider in order to obtain high yield bio-oil and gas from textile waste using this thermal process in the same sense that energy savings will be achieved in textile manufacturing industries [21].

In this research, the objective was to study, through pyrolysis processes, the energy potential of three industrial residues of vegetable (CW, SFW) and animal (W) origin and derived from the textile sector. To this end, conventional and flash pyrolysis were carried out at 500 °C and 750 °C. The solid (bio-char), liquid (bio-oil) and gaseous fractions obtained in the pyrolysis processes were extensively characterised to assess the potential of the textile residues as a fuel source in the bioenergy sector. The investigation was completed with a study of the thermogravimetric behaviour of the residues and its kinetic study, in addition to the identification of yields for the various pyrolysis fractions.

## 2. Experimental

### 2.1. Materials

A prestigious Spanish business group, Textil Santanderina S.A, provided three textile remnants of vegetable and animal origin. It works for well-known international fashion firms and which focuses mainly its production in weaving and finishing of textile products. In its facilities, all the spinning mills, weaving mills, bleaching/mercerizing, and dyeing/finishing are processed. Thus, the wastes analysed in this study were the following, Fig. 1:

- *Card waste (CW)*. This residue is generated in the first cleaning of the cotton and can contain seeds, tobacco, cotton, branches, leaves and cross contamination acquired during harvesting among other possible residues. It can be produced as such or ground, then called card waste dust.
- *Short fibre waste (SFW)*. Rejection consisting of short spinning that comes from batting, carding and combing of cotton fibres.
- *Wool (W)*. Wool discarded in a first selection within the triage of the textile industry.

After a random sample, raw materials were directly sampled from the industry in accordance with the standard ISO 24153 2009. When the analysis demanded it, these materials were milled with a Fritsch™ mill Model P-19 instrument to a 1 mm particle size and later using a Retch™ ball mill model MM200, particle diameters of 0.2 mm were obtained.

The samples were identified with an appropriate nomenclature. The first part of the name is related to the type of waste (CW, SFW and W, for card waste, short fibre waste or wool waste, respectively) and the second part includes the pyrolysis temperature (500 °C or 750 °C) as well as the type of pyrolysis (P or F: conventional or flash pyrolysis).

### 2.2. Samples characterisation

#### 2.2.1. Chemical characterisation

A LECO CHN-2000 equipment was used to determine the concentrations of carbon (C), hydrogen (H), and nitrogen (N). With a LECO S-144-DR instrument, the Sulphur (S) concentration was determined (LECO Corporation, Groveport, Ohio, United States). Oxygen (O) content was estimated by difference. On a TGA 701 LECO, moisture and ash content were assessed in relation to proximate analysis. The UNE 32019 standard for volatile matter was met, and the fixed carbon (FC) content was computed using the difference. The adiabatic IKA-calorimeter C4000 was used to perform the high heating values (HHV) (IKA, Germany). Regarding the elemental analysis of the bio-oils obtained, a LECO CHNS-932 automatic equipment was used. The oxygen analysis of these oils was determined in a LECO VTF-900 system. Analysis was done by triplicate.

HHV of the various fractions (bio-char, bio-oil, and gas) was estimated using the elemental analysis data. By doing so, Doulong-Petit [22], Eq. (1), was employed to estimate the HHV for bio-chars. Bio--oils calorific values were estimated following Beckman [23], Eq. (2), Friedl [24], Eq. (3) and IGT (Institute of Gas Technology) [25], Eq. (4), formulas. The HHV of the bio-oils calculated with Eq. (4) was made without considering their ash content. Similar to this, a number of material and energy balances were required to determine the HHV for the gases.

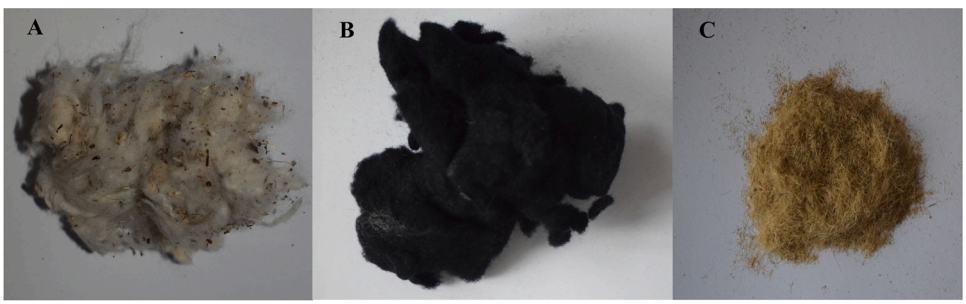


**Fig. 1.** Textile samples analysed. (A) Card Waste, CW; (B) Short Fibre Waste (indigo dyed fibre), SFW and (C) untreated Wool (W).

$$HHV\ (kcal/kg) = 8140\ C + 34{,}400\ (H - O/8) + 2220\ S \quad (1)$$

$$HHV\ (MJ/kg) = 0{\cdot}352C + 0{\cdot}994H + 0{\cdot}105{\cdot}(S - O) \quad (2)$$

$$HHV\ (MJ/kg) = (3{\cdot}55\ C^2 - 232\ C - 2230\ H + 51{\cdot}2\ H + 131\ N + 20{,}600) \times 10^{-3} \quad (3)$$

$$HHV\ (MJ/kg) = (341\ C + 1323\ H + 68\ S - 15{\cdot}3\ A - 120\ (O + N)) \times 10^{-3} \quad (4)$$

C, H, S, A, O and N are the mass fractions (%) of the carbon, hydrogen, sulphur, ash, oxygen and nitrogen contents, respectively. In Doulong-Petit equation the data is not in %.

A portion of the CW and SFW bio-oils were dragged with dichloromethane and a portion with acetone during the collection process. This indicated the non-polar and polar character of the compounds present. However, W samples were dragged exclusively with dichloromethane. For the elemental analysis of the oils, the polar and non-polar parts were combined.

#### 2.2.2. Thermogravimetric analysis and characteristic indexes

A TGA instrument Q 5000IR was used for thermal analysis. With the help of this device, sample weight can be continuously measured as a function of time or temperature. In a titanium crucible, milled textile samples were heated while being surrounded by a nitrogen atmosphere, weighing between 14 and 25 mg. A flow of 10 mL/min of $N_2$ was used for heating, and the temperature was increased by 30 °C/min until it reached 750 °C. This way, thermogravimetric (TG) profiles were acquired. It is recommended to create these TG profiles to distinguish between the various stages (DTG profiles). They enabled the identification of significant parameters, including the temperature at which each stage occurs and the mass loss.

A series of comprehensive indexes were used as a criterion for pyrolysis release characteristics depiction. $T_o$ estimate these indexes, temperatures for ignition ($T_i$) and burnout ($T_b$) are required. $T_i$, which can be calculated using the Li et al. [26] protocol, is defined as the lowest temperature at which a fuel will spontaneously ignite in an environment without an external source of ignition [27]. Its degree of reaction is indicated by the burnout parameters. $T_b$ refers to the temperature at which the fuel is almost completely consumed. This way, it corresponds to the temperature value, once the maximum DTG value has been exceeded. For this work, the final stage temperature was considered as $T_b$. There are fewer combustible components in the fuel at higher burnouts [28]. In addition, several parameters were estimated to know how well the fuels burned.

Based on the expressions already present in the current literature for the various thermal processes, authors obtained the pyrolysis characteristic index (P), stability index ($R_w$), $H_f$, and D indexes using the above-mentioned factors [29–31]:

$$P = \frac{DTG_{max} \cdot DTG_{mean}}{T_i^2 \cdot T_b} \quad (5)$$

$$H_F = T_p \cdot \ln\left(\frac{\Delta T_{1/2}}{DTG_{max}}\right) \cdot 10^{-3} \quad (6)$$

$$D = \frac{DTG_{max} \cdot DTG_{mean} \cdot M}{T_i \cdot T_b \cdot \Delta T_{1/2}} \quad (7)$$

$DTG_{max}$ is the maximum rate (%/min), $DTG_{mean}$ the average rate (%/min) considering as start and end the 10 % of the $DTG_{max}$, $T_i$ is the ignition temperature (℃), $T_b$ is the burnout temperature (℃), $T_p$ is the peak temperature (℃), M is the pyrolysis mass loss for the stage temperature interval (%) and $\Delta T_{1/2}$ is the temperature range (DTG ≥ 0.15 %/min) for stage.

An improved thermal property has a higher P value [29]. Related to $H_F$ parameter, it describes the rate and the intensity of the thermal process. A smaller value reflects better properties [30,32]. To further evaluate the pyrolysis characteristics, the comprehensive pyrolysis characteristic index (Index D) was developed [31,33]. The degree of pyrolysis difficulty is represented by index D. The value of index D is significantly influenced by the initial decomposition temperature, reaction time, and maximum rate. A more active material decomposition and a more intense pyrolysis reaction are indicated by high values of D [34].

### 2.3. Pyrolysis process

An original experimental set-up already employed in [35,36] was used. The experimental device has been extensively detailed in these works. In addition, Fig. 2 has been included in the work for a better understanding of the pyrolysis processes. The experimental setup consists of a horizontal tubular furnace with a quartz reactor, a $N_2$ mass flow controller, a cooling condenser, a Tedlar bag for gas collection and a stick with mechanical device to introduce the crucible in the oven (Fig. 2).

The sample weight used in each pyrolysis experiment ranged from 2 to 5 g for all industrial textile wastes. Samples were placed in an alumina crucible for both flash and conventional pyrolysis (Sigma-Aldrich, USA).

The conventional pyrolysis experiment was carried out using a $N_2$ flow of 100 mL/min, a heating rate of 25 °C/min, a pyrolysis temperature of 500 °C or 750 °C, and a residence time of 1 h at final temperature. Initially, the crucible with the sample was placed in the geometric centre of the quartz reactor installed in the furnace; then, a nitrogen flow was passed for half an hour to make the atmosphere inside the reactor inert. After that time, the oven-heating program started. The gas and bio-oil fraction were collected in the temperature interval between 200 °C and 550 °C (temperature range in which biomass devolatilization is shown by thermogravimetric analysis).

In flash pyrolysis, the oven (without the sample) was heated to the final pyrolysis temperature (500 °C or 750 °C). A $N_2$ flow of 100 mL/min was passed during all of the experiment. Once the oven reached the pyrolysis temperature, the sample was instantly introduced into the oven by a mechanical mechanism. The gas and bio-oil fraction were collected for 10 min after introducing the sample in the oven. After that time, the sample was removed from the oven.

The wool residue (W) has a high nitrogen content, 17.1 %, which is why argon was used as inert gas in the pyrolysis processes, instead of nitrogen.

Dichloromethane ($CH_2Cl_2$) was used to extract the biooils from the condenser. For CW and SFW samples, in addition to dichloromethane, acetone was also used to completely remove all bio-oils from the condenser. The organic solvent solution and bio-oil fraction was passed through a column packed with anhydrous sodium sulphate ($Na_2SO_4$), to remove moisture from the bio-oil. Subsequently, the bio-oils and organic solvent solutions were placed in glass containers, sealed and kept refrigerated at − 3 °C (optimal conditions for subsequent chromatographic analysis).

### 2.4. Chromatographic analysis

A GC System 7890 A chromatograph was used to carry out the chromatographic examination of the gases fraction (Agilent Technologies, Wilmington, DE, USA). The flame ionisation detector (FID) was set up to analyse hydrocarbons with one to five carbons, with components with six and more carbons aggregated and measured in a single peak at the start of the study. Helium was used as the reference gas or mobile phase in a thermal conductivity detector (TCD) setup to analyse the fixed gases. The second TCD was used for the $H_2$ analysis, with $N_2$ serving as the reference gas.

The chromatographic examination of the bio-oil was performed using an Agilent 7890 A chromatograph and a 5975 C mass spectrometer (Agilent Technologies, Wilmington, DE, USA). The chemicals were separated using an HP-5MS capillary column (Agilent Technologies, Wilmington, DE, USA) (5 % phenyl-methylpolysiloxane).

For the identification of compounds, the NITS 08 and WILEY 7 N

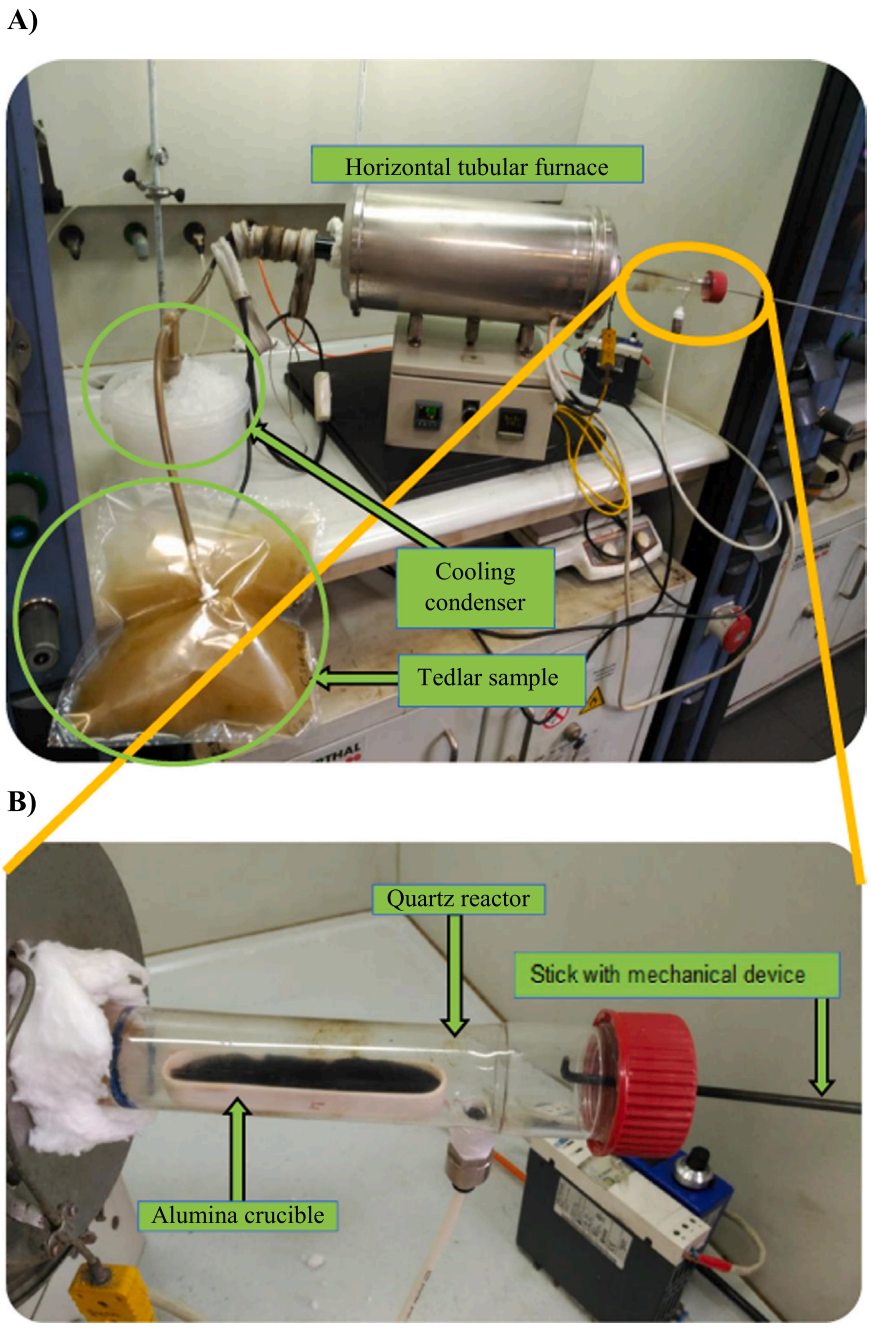


**Fig. 2.** A) Pyrolysis set up schema. B) Cold part of the quartz reactor and device for mechanical introduction of the sample.

libraries were used. There are many organic compounds in bio-oils, and those whose peaks had areas greater than 0.2 % were identified in the chromatograms. The discovered compounds were categorised into families: non-aromatic and aromatic, distinguishing the latter between aromatics without benzene rings and aromatics with 1, 2, 3 or 4 benzene rings.

### 2.5. SEM-EDX

An energy-dispersive X-ray analysis system-equipped scanning electron microscope, the ZEISS Model DMS-942 (ZEISS, United States), was used to investigate the textile samples and the bio-char produced by conventional and flash pyrolysis (Link-Isis II). Iridium was applied to the samples before inspection to lessen their charge and enhance the SEM images. For this, an Emitech K575X instrument was used.

## 3. Results and discussion

### 3.1. Chemical characterisation

Textile samples characterisation results appear in Table 1. A slight observation reveals a significant difference between the W and CW-SFW values. Both types of materials had their potential as energy sources. In fact, the results of the CW and SFW analytical studies were consistent with a number of raw materials whose thermal degradation has already been researched and reported [37,38]. Samples carbon (C) content (~ 47 %) was higher than the present in bibliography for agricultural biomass residues [39] and so like woody biomass sources [40]. This profile suggests a favourable future for this energy material conversion, although coals' carbon concentration is far away [41]. The behaviour of nitrogen (N) and hydrogen (H) values was similar. Wool stood out from

**Table 1**
Ultimate, proximate analysis and calorific values for textile residues.

| | Ultimate analysis | | | | | | Proximate analysis | | | | | |
|---|---|---|---|---|---|---|---|---|---|---|---|---|
| | C[a] (%) | H[a] (%) | N[a] (%) | S[a] (%) | Cl[a] (%) | O[ab] (%) | Moisture (%) | Ash[a] (%) | VM[a] (%) | FC[ab] (%) | HHV (MJ/kg) | LHV (MJ/kg) |
| CW | 45.2 ± 0.5 | 5.8 ± 0.2 | 1.2 ± 0.2 | 0.08 ± 0.01 | 0.18 ± 0.00 | 44.3 ± 0.6 | 8.2 ± 0.3 | 3.5 ± 0.3 | 79.1 ± 0.6 | 17.4 ± 0.5 | 17.40 ± 0.42 | 16.18 ± 0.30 |
| SFW | 47.1 ± 0.3 | 6.1 ± 0.1 | 2.0 ± 0.2 | 0.09 ± 0.01 | 0.01 ± 0.00 | 43.5 ± 0.3 | 8.6 ± 0.2 | 1.2 ± 0.1 | 81.2 ± 0.4 | 17.6 ± 0.7 | 18.74 ± 0.53 | 17.46 ± 0.29 |
| W | 48.6 ± 0.4 | 6.3 ± 0.1 | 17.1 ± 0.6 | 2.41 ± 0.08 | 0.12 ± 0.00 | 20.9 ± 0.2 | 12.7 ± 0.4 | 4.7 ± 0.5 | 79.5 ± 0.3 | 15.8 ± 0.0 | 20.67 ± 0.34 | 19.52 ± 0.27 |

[a] Dry basis.
[b] Determined by difference.

other materials in terms of its nitrogen content (17.1 %). As is well known, besides carbon element, wool fibre contains a large amount of nitrogen and sulphur element [42]. Regarding oxygen, it is also an important parameter in the HHV calculation. CW and SFW samples had similar O values (~ 44 %) which denoted lower HHV in comparison with W, that had lower O data (20.9 %). As the sulphur and chlorine was concerned, although the main problems appear with high levels for these elements under combustion thermal process, these elements as well as their reaction products may be related to heating equipment corrosion and damaging emissions. This way, low values for both elements are desirable. CW (0.08 % S) and SFW (0.09 % S) have lower sulphur values than W (2.41 %). CW and SFW sulphur values are so close to pyrolysis oil [43] and the great majority of the biomass sources [37,44,45]. Chlorine is yet another element that reduces the yield of a particular fuel [46]. The results obtained for this parameter, lower than the typical ones for agricultural wastes, reflected that it would not a be a problem when pyrolytic process was carried out [47].

On the other hand, low values for moisture and ash are recommended for pyrolysis. When compared to W, CW and SFW residues have lower values for these two parameters. This is true because wool is a protein fibre that is hydrophilic. Wool possesses a -CO.NH- group in its protein, which may draw moisture from the surrounding air. When its environment changes, it has the ability to both absorb and expel moisture vapour. Wool absorbs roughly 13–18 % of moisture under typical

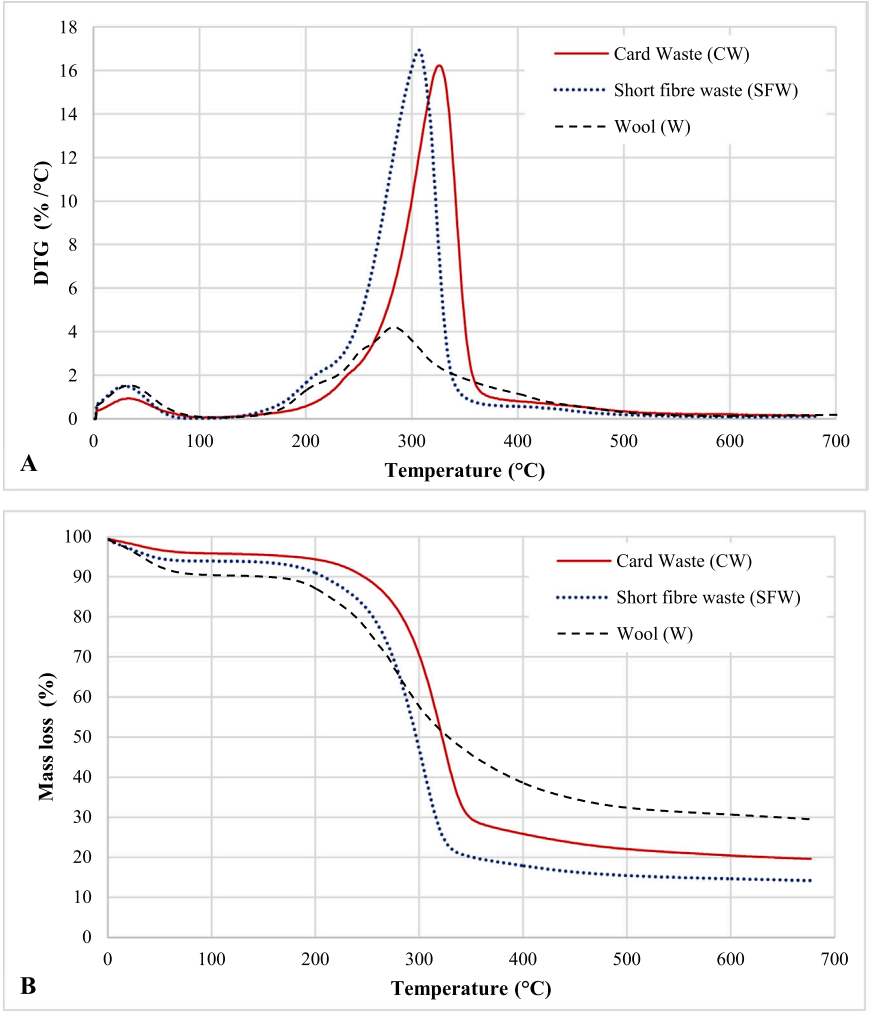


**Fig. 3.** Textile samples DTG (**A**) and TG (**B**) profiles.

atmospheric conditions. [48], values in line with the W selected for this work (12.7 %). In consequence, several desorption of moisture methods is pursued when wool is used [49]. Samples ash content (lower than 5 %) had have acceptable values for a pyrolytic thermal process when compared with literature [40,50].

Finally, and linked to HHV, CW and SFW both produced findings (~18 MJ/kg) that were similar. They were less expensive than fossil fuels [51] and comparable to woody biomass [52]. However, wool shows a 20.67 MJ/kg result, which is substantially higher than that of biomass used for energy purposes [53] and higher even than hydrochar [54]. The average HHV results for textile residues were frequently higher than those for wood, lignite, food, and leather wastes [55].

Hence, and contrary to what happens with other waste derived from the textile industry, such as the like the textile dyeing sludge, TDS, (with a high moisture and ash contents as well as low calorific value) [56], the materials selected for this study have a promising pyrolytic behaviour.

### 3.2. Textile samples TGA profiles. Characteristic parameters and indexes

The thermogravimetric TG and DTG profiles are shown in Fig. 3 together with the characteristic parameters in Table 2**.** Pyrolysis patterns were obtained by TGA up to 650 °C. Literature [57] states that the volatiles are primarily lost up to 500 °C, this temperature was chosen. The mass loss rates for all the samples from 500 °C forward are very stable, as shown in Fig. 3**.B,** hence not much further weight loss was anticipated above 650 °C.

Profiles here obtained were so like literature results for textile fabrics/materials/waste [58]. Initial, main, and char decomposition are the three stages of pyrolysis for textile samples. The temperature, rate, and weight loss of each stage can be calculated using the TGA curve. Due to moisture loss, the fibres initially experience some physical changes and a small weight variation when the temperature range is below 100 °C. In this instance, the cellulose is most severely harmed in the amorphous region of the polymers. Between 150 and 380 °C, the primary pyrolysis stage takes place. The weight loss is rapid and significant at this point. The primary components of cotton, cellulose and hemicellulose, are disintegrated during this time. Additionally, these biopolymers are linked to additional transformations that start at 415 °C [59]. In this stage, most pyrolysis products are created (being L-Glucose one of the major products, together with all kinds of combustible gases). When the temperature is higher than 430 °C, char pyrolysis takes place. The charring and dewatering reactions compete with the production of L-glucose during this process, with the latter two reactions being more pronounced. As the products of decomposition contain an increasing amount of carbon, charred residues are produced [60].

Comparing these materials with other possible residues of the textile value chain, such as the textile dyeing sludge (TDS), results here obtained denoted higher mean DTG values. For TDS, $DTG_{max}$ values were between 1.5 %/min [61] and 3 %/min [62] whereas this same parameter was above 16 %/min in the case of CW and SFW. Note how for TDS there was a final residue close to 50 %, while in this study the values for this parameter are always less than 30 %, Fig. 3B.

Regarding characteristic profiles and indexes, Table 2, it can be stated that CW and SFW materials had better pyrolytic behaviour than W. With a $DTG_{max}$ value of 4.216 %/min for wool, it was far from the more than the 16 %/min results for the other materials. In the case of W, the main region of thermograms was also much wider, indicating that the mass release was not only lower but also occurred more gradually given the conditions. In contrast, weight release for CW and SFW materials were faster than W, as depicted in the shortest and narrowest DTG profiles, Fig. 3A. The SFW final residue (14.18 %) was less than half of W value (29.31 %); which reported a better SFW energy use. The above assumptions were reaffirmed with the characteristic indexes. Looking for high values for P, and D, as well as low values for Hf, it was again confirmed that the best pyrolytic performance was for CW and, especially, SFW. The values of the characteristic index, P, were, for the three cases, higher than $2{\cdot}10^{-7}$, which indicates a good thermal behaviour of the materials [63]. The few or no publications related to the pyrolysis of this type of materials make it difficult to compare these indexes. Nevertheless, for textile materials, the values of P index were higher than those obtained by the same authors for biomass samples [64]. D index results for CW and SFW, in contrast, were better than those for paper mill sludge and municipal solid waste [33].

### 3.3. Pyrolytic process

#### 3.3.1. Yield

The yields obtained for each fraction of pyrolyzed textile material at 500 and 750 °C during flash and conventional pyrolysis appear in Fig. 4. These temperatures were chosen based on previous thermogravimetry trials. In the first place, there is a generalised performance in which, for each material, the solid fraction (bio-char) was the one that varied the least regardless of the temperature increase and the pyrolysis type. W sample was the one that, under any circumstances, showed a higher biochar content. Secondly, and with the exception of flash pyrolysis at 750 °C (where the gas fraction prevails), for the rest of the tests, the bio-oil fraction predominated. The largest amount of bio-oil was obtained for SFW-500P, where more than half of what was obtained in the pyrolysis, 55.12 %, was bio-oil. Regarding gas fraction, yield results showed that, flash pyrolysis at 750 °C was the thermal process linked to the higher gas fraction for all the textile results here studied, focusing on the SFW-750F with a 55.53 %. This contrast with similar research made by the authors concerning pomegranate (*Punica granatum* L.) peel wastes, where at these same conditions and with the same equipment, liquid fraction stood out above the rest [35].

When compared with herbaceous biomass, like sugarcane bagasse, results were different according to the pyrolysis types. For slow pyrolysis at approximately 750 °C, textile bio-oil values were higher than the obtained for here studied, focusing on the SFW-750P with a 41.42 %. This behaviour, the above, not maintained for the same temperature at

**Table 2**
Textile samples TGA pyrolysis profiles characteristic parameters and indexes.

| Sample | $DTG_{max}$ [a] %/min | $TDTG_{max}$ [b] °C | Main region[c] °C | Final Residue[d] % | $T_i$[e] °C | $T_b$[f] °C | P[g] | $H_f$[h] | D[i] |
|---|---|---|---|---|---|---|---|---|---|
| CW | 16.223 | 346.55 | 141–379 | 19.61 | 305.07 | 379 | 3.48E-06 | 1.188 | 9.62E-05 |
| SFW | 16.937 | 330.28 | 165–362 | 14.18 | 285.62 | 362 | 4.40E-06 | 1.026 | 1.88E-04 |
| W | 4.216 | 300.16 | 166–497 | 29.31 | 249.08 | 497 | 2.54E-07 | 1.370 | 1.73E-05 |

[a] $DTG_{max}$: maximum value of DTG (%/min).
[b] $TDTG_{max}$: Temperature at which $DTG_{max}$ is achieved (°C).
[c] Main region: Temperature interval for the pyrolysis main region (°C).
[d] Final residue: Mass remaining at the end of the pyrolytic profiles, ~700 °C, (%).
[e] $T_i$: ignition temperature (°C).
[f] $T_b$: burnout temperature (°C).
[g] P: characteristic factor ($\%^2/(min^2 \cdot °C^3)$).
[h] $H_f$: ignition parameter.
[i] D: comprehensive index ($\%^3/(min^2 \cdot °C^3)$).

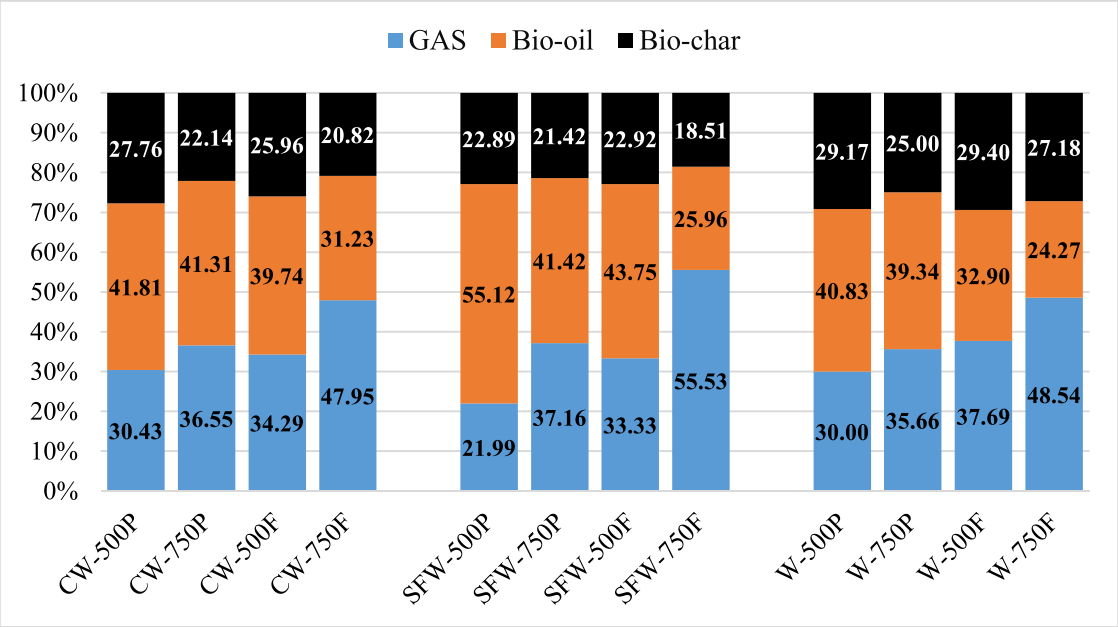


**Fig. 4.** Yield of gas, bio-oil and bio-char fractions in the different pyrolytic processes.

flash pyrolysis. Under these conditions, the percentage of liquid fraction increased notably for biomass (up to 50.89 %) [65] and decreased for textiles.

On the other hand, conventional pyrolysis fractions percentages were so similar to the presented for lignocellulosic biomass [66]. However, when an analogy is made with this same raw material for fast pyrolysis at 500 °C, this research textile samples had higher bio-char and gas values but considerably lower bio-oil yields (~ 38 ± 5 % vs ~70 %) [67].

Considering all the particularities about this section, the obtained results verified the possibility of conversion of the textile samples selected through conventional and flash pyrolysis processes in different fuels (bio-char, gas, bio-oil).

### 3.3.2. *Gas fraction*

Fig. 5 shows the gas chromatographic analysis for the different pyrolysis processes and textile samples. Several differences were observed. While for W, regardless of the type of pyrolysis and temperature, the most emitted gas was $O_2$ (>90 %), for SFW this predominant gas was the CO (with values above 45 % in all cases). Regarding SFW, $CO_2$ and CO were the gases emitted to a greater extent (depending on the type of pyrolysis and temperature).

For all three materials, a greater variety of gases were emitted during flash pyrolysis. In fact, for CF and SFW materials, only three gases were detected in conventional pyrolysis, CO, $CO_2$ and $O_2$. However, many other gaseous species appeared in the flash pyrolysis (noteworthy: methane, ethane, ethylene, propane and propylene). In the same way, all of the samples examined show a significant increase in the methane and hydrogen content as the temperature of the flash pyrolysis rises (from 500 to 750 °C). Methane went from 1.32 % in CW-500F to 13.94 in CW-750F and $H_2$, under the same circumstances, increased from 0.28 % to 11 %. The analogous percentages for SFW-500F and SFW750F were 3.73–14.23 % for methane and 0.29–10.87 % for hydrogen.

Raw materials chemical composition (Section **3.1**) greatly influenced the components presented in the syngas fraction. Thus, the higher SFW carbon content (47.1 %) when compared to CW (45.2 %), was consequently reflected in a higher CO level within gas fraction for all the pyrolysis conditions (CO values for SFW are always higher than 43 %, whereas CO percentages for CW were not, in any case, higher than 40 %). CO SFW content was similar than the achieved for the same authors of this work for biomass samples [36].

Chromatographic gases obtained from this fraction were in line with the few published works on the characterisation of the pyrolysis gases derived from these materials [68]. In particular, and it is also corroborated in this research, when a pyrolytic process under $N_2$ is carried out, there was a clear trend characterised by the emission of small amounts of $H_2$, $CH_4$, and $C_2H_4$, while CO levels are higher [69,70].

The HHV values for the gases obtained through conventional and flash pyrolysis of industrial textile wastes varied significantly for both. The highest values of HHV were for the gases obtained by high-temperature flash pyrolysis due to the presence of higher flue gas (CO-$H_2$-$CH_4$-light hydrocarbons) and lower $CO_2$ contents in these conditions; gaseous components that, in isolation, provide greater energy to the final gas mixture. The pyrolysis gas obtained from the wool waste (W) showed much lower HHV values (0.01–1.30 MJ/Kg) than pyrolysis gases of cotton waste (1.44–13.18 MJ/Kg and 4.19–15.34 MJ/Kg, from CW and SFW wastes, respectively), which can be due to its high $O_2$ content. This element did not oxidise further and, therefore, it did not provide calorific value to the final gas fraction. The SFW-750F gas reached the highest HHV value (15.34 MJ/kg). Although CW-750F HHV result was also acceptable (13.80 MJ/kg), SFW textile residue, under flash pyrolysis, released a greater quantity of gases such as methane, ethylene, propylene and, above all, CO, which influenced the higher HHV value.

Both conventional and flash pyrolysis HHV results were in line with previous studies undertaken by the authors following the same or similar conditions [35,36]. Similarly, and despite being further away from the HHV connected to fossil fuels [71], results here obtained for CW and SFW were acceptable according to the values obtained for different materials recently analysed [72,73].

To sum up, the gas fraction of CW and, especially SFW, during flash pyrolysis together with their high HHV, advised us to employ these gases as fuels. Table 3.

### 3.3.3. *Bio-oil fraction*

The cotton residue-derived bio-oil samples, CW and SFW, exhibit two distinct phases: an oily phase and an aqueous phase. These phases were separated and characterised independently by GC-MS. While, the pyrolysis bio-oils derived from wool residue, W, only had an oily phase. This difference observed in the pyrolysis bio-oils obtained from the

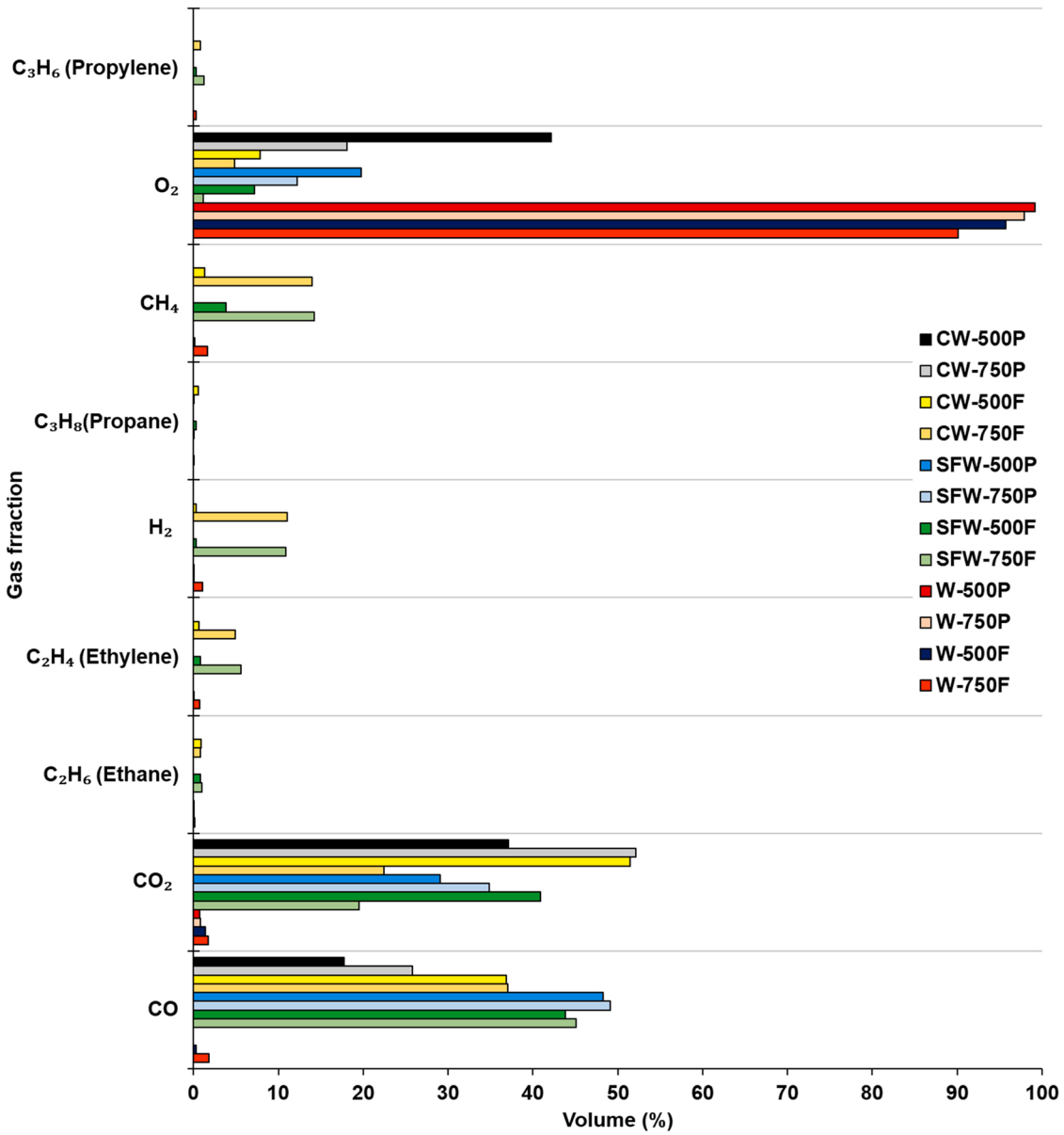


**Fig. 5.** Composition of the gas fraction for the different textile samples and pyrolysis processes.

**Table 3**
Textile samples HHV for the gas fractions obtained under the different pyrolysis processes.

| Textiles samples | HHV (MJ/kg) |
|---|---|
| CW-500P | 1.44 |
| CW-750P | 2.03 |
| CW-500F | 4.32 |
| CW-750F | 13.80 |
| SFW-500P | 4.19 |
| SFW-750P | 4.22 |
| SFW-500F | 6.15 |
| SFW-750F | 15.34 |
| W-500P | 0.01 |
| W-750P | 0.03 |
| W-500F | 0.18 |
| W-750F | 1.30 |

textile waste may be due to the plant origin of the CW and SFW samples compared to the animal origin of the W sample.

For each type of pyrolysis and each textile waste considered, Fig. 6 shows the proportion of organic compounds identified in the oily phase. For each type of sample and pyrolysis, the production of aromatic and non-aromatic biooils can be compared in the figures. Additionally, the distribution of aromatic organic compounds found in biooils is investigated based on the number of benzene rings (0, 1, 2, 3 and 4).

For all the textile residues considered, the flash pyrolysis at 750 °C stands out from the rest of the pyrolysis studies because it is the one that produces the most aromatic oils; specifically, in the case of SFW-750F, 96.84 % are aromatic bio-oil compared to 0.54 % non-aromatic bio-oil (2.62 area % unidentified compounds). Similar results were obtained in the study by Pérez et al. on conventional and flash pyrolysis of the pampa grass [36]. The 750F pyrolysis differs from the rest of the pyrolysis studied because it has a higher cracking capacity for all of the samples studied, producing significantly more aromatic oils than the rest of the pyrolysis, regardless of sample. In any case, all of the pyrolysis investigated produced more aromatic oils, with differences between the various families of aromatics produced by each type of waste and each type of pyrolysis generated.

Thus, in the two conventional pyrolysis studies (500 and 750), Fig. 6. B, there are essentially no differences in the production of non-aromatic

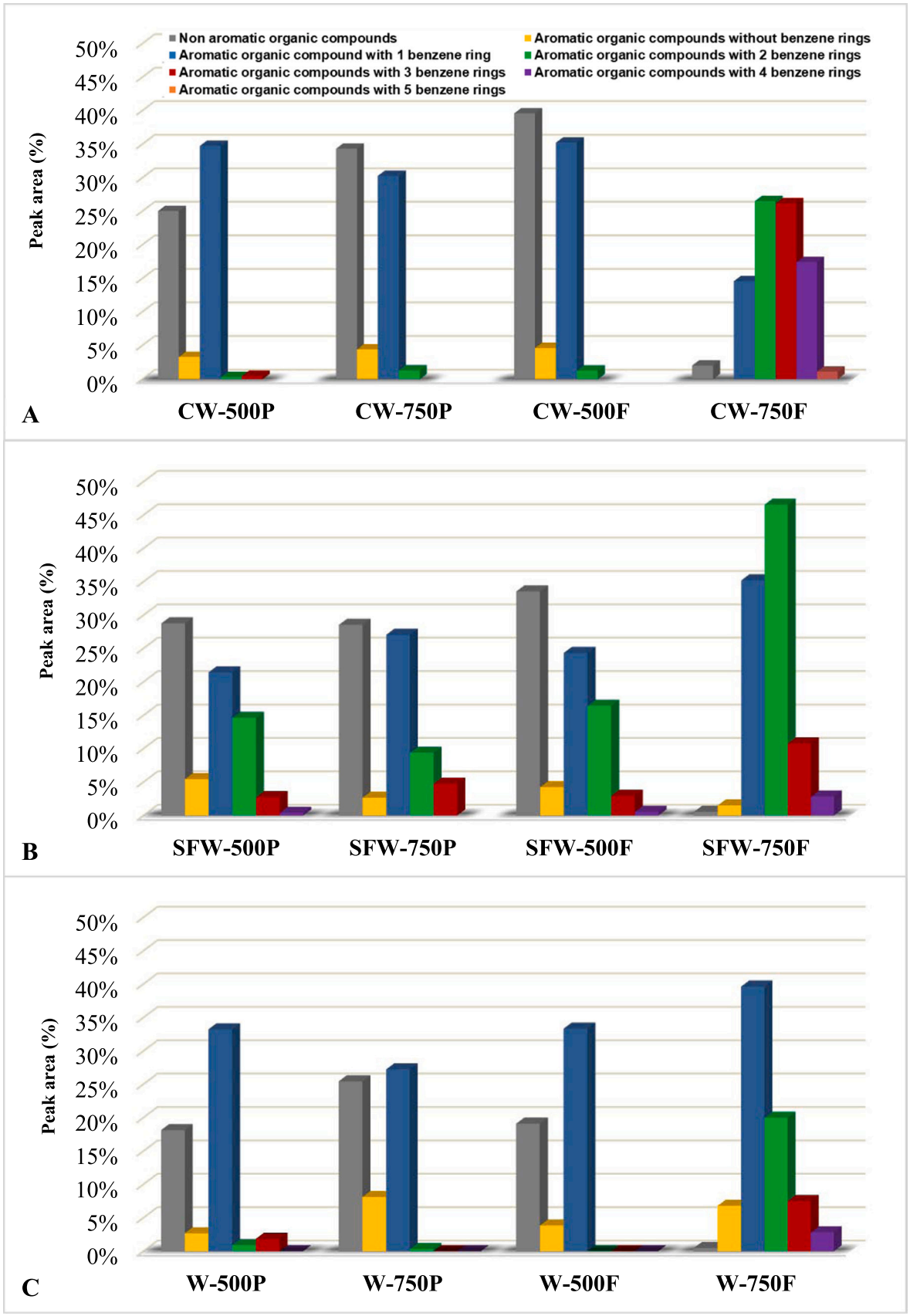


**Fig. 6.** Composition of the Bio-oil fraction for the different textile residues and pyrolysis processes. (A) CW, (B) SFW and (C) W.

oils, but there are differences in the production of aromatics with one benzene (higher in SFW P750) and aromatics with two benzenes (minor in SFW P750). Of the non-aromatic compounds that are present in the SFW-500P, SFW-750P, and SFW-500F bio-oils, the presence of cyclic ketones stands out with 10–12.6 % peak are values. N-hexadecanoic and octadecanoic acids are present in similar (8–13 % peak area). Lactones are present at 5–8 %. The SFW-750F bio-oils do not contain the aforementioned compounds.

In relation to the aromatic compounds with a benzene ring present in SFW-500P, SFW-750P, and SFW-500F, phenol and its derivatives (9–12 %) and indole and its derivatives (2–8 %) stand out. However, in the SFW-750F bio-oil, phenol and its derivatives constitute only ≈ 5 %, while indole derivatives increase to 12.75 % and specifically the signal of the indole compound (9.82 %), to a retention time of 17.05 min, is the most intense in the chromatogram. All bio-oils obtained by pyrolysis of SFW differ from those obtained from CW and W because, regardless of the pyrolysis conditions, they always contain PAHs. Comparatively, the bio-oils obtained by flash pyrolysis of pampas grass were mainly composed of PAHs, while the bio-oils obtained from their conventional pyrolysis practically do not contain PAHs, as in the case of CW and W bio-oils [36].

SFW-750F has a high content of aromatic compounds with several benzene rings, highlighting, among others, compounds derived from naphthalene, fluorene, carbazole, phenanthrene, anthracene, fluorantheum, fluorene or pyrene. The highest concentration of PAHs with two benzene rings (>45 %) occurs in SFW-750F, Fig. 6**.**

Despite the fact that CW and SFW residues come from the same source, there are distinct differences in the makeup of bio-oils. Of the non-aromatic compounds present in bio-oils CW-500P, CW-750P, and CW-500F, the presence of cyclic ketones also stands out, reaching maximum values of up to 21.5 % in CW-750P; n-hexadecanoic and octadecanoic acids are also present, but in smaller quantities (3–5 %) and with different proportions between them, always dominating n-hexadecanoic; finally, the lactones are in 3–6 area %. Gamma-Sitosterol (2.5–3 %), a chemical compound that belongs to the class of phytosterols, which are sterols that are naturally present in plants, is present in these oils, which is consistent with the oils' botanical origin. In the study, this substance wasn't discovered in any other oils. CW-750F also does not contain cyclic ketones and lactones. Aromatic compounds with a benzene ring present in CW-500P, CW-750P, and CW-500F bio-oils account for 30–35 %, while in SFW-500P, SFW- 750P, and SFW-500F account for 21–27 area %, Fig. 6**.**

In bio-oils CW-500P, CW-750P, and CW-500 there is a clear dominance of phenol and derivatives (23–28 %), while indole derivatives are practically absent (<2 %). In CW-750F, phenol and its derivatives are reduced to ≈ 5 a %, and indole derivatives increase slightly to 3.14 %, a value four times lower than that of SFW-750F bio-oil (12.75 %). The bio-oil with the highest concentration of PAHs with 3 and 4 benzene rings is CW-750F, which also stands out for its high PAH content. Thus, for example, phenanthrene/anthracene and its derivatives are 17 % in CW-750F vs. 4.6 % in SFW-750F, or pyrene and its derivatives with 10.5 % in CW-750F vs. 1 % in SFW-750F.

W is distinguished by the production of aromatics at 1 benzene, Fig. 6C, which is higher at 750F and similar for the two pyrolysis experiments conducted at 500 °C. Conventional pyrolysis and low temperature flash pyrolysis of W generate bio-oils (W-500P, W-750P, W-500F) with non-aromatic compounds such as cyclic ketones (12–15 %) but without traces of lactones and acids. W-750F barely contains cyclic ketones (0.5 area %). W-500P, W-750P and W-500F contain almost no HAPs, as is the case with CW-500P, CW-750P, and CW-500F and contrary to what is obtained with SFW-500P, SFW-750P, and SFW- 500F. PAHs were identified in W-750F and this bio-oil stands out from all the bio-oils in the study for having the highest amount of aromatic organic compounds of a benzene ring (≈40 %).

The analysis of the aqueous phase of the derived SFW samples shows a different composition than that found in the oily phase; in general PAHs have not been detected; This phase is notable for being primarily composed of non-aromatic compounds, aromatic compounds without benzene, and aromatic compounds containing benzene. Specifically, in the aqueous phase of SFW flash pyrolysis bio-oils at 750 °C, aromatic compounds with a benzene ring stand out with 42.65 % of the detected material.

Also, the composition of the aqueous phase of CW differs in composition from its oil phase; These phases of the CW bio-oils have high contents of non-aromatic compounds, reaching 46 % of the chromatographed material in what is obtained by conventional pyrolysis at 500 °C.

For its part, Table 4 shows the bio-oils ultimate analysis and high heating values (HHV). For all the samples, C content was higher under flash pyrolysis at 750 °C. Under this particular condition, CW and SFW values were higher than W. Considering that C is one of the main elements for energy obtention [74], the bio-oils for both samples were really interesting as was corroborated in their associated HHV results. H percentages were so similar being somewhat higher in the case of wool. W oil had a large percentage of N (~12 %). This fact was due to the high content of this element in the original raw material (Table 1). CW and SFW oils have high oxygen content (up to 33 %) except those obtained by F750 which values as low as 6.53 %. In the case of wool oils, the values range between 8 % and 16 % with the lowest value for that obtained by F750. Regarding HHV, the formulas used denoted were very similar in the values of HHV. This indicated, on the one hand, that the ash content (2–6 %) practically did not influence the final values and, on the other hand, the validity of the use of any of these expressions. As previously stated, 750 °C temperature flash pyrolysis bio-oils were the ones that obtained the best results, due to their higher carbon content, highlighting SFW-750F (34.15MJ/kg). These results, despite not being as high as the HHV for diesel or conventional fuels (> 45MJ/kg) [75], were in line with biomass sources [76,77] and alternative biodiesel [78], denoting their acceptable thermal utilisation.

Despite the high HHV value of SFW-750F bio-oil, its high content of PAHs greatly restricts its use for energy purposes (combustion). However, in the chemical industry most PAHs, such as phenanthrene, are used to make plastics, pesticides, dyes, explosives, etc. In the plastic industry, synthetic tanning agents and phenanthrene, under high temperature and high pressure, can undergo hydrogenation to get hydrophenanthrene, being the fuel of senior jet aircraft [79].

**Table 4**
Bio-oils analysis and calorific values.

| | Ultimate analysis | | | | HHV (MJ/kg) | | |
|---|---|---|---|---|---|---|---|
| | C[a] (%) | H[a] (%) | N[a] (%) | O[a] (%) | Beckman | Friedl | IGT- no ash |
| CW-500P | 60.70 | 6.60 | 1.45 | 29.21 | 24.86 | 25.58 | 25.75 |
| CW-750P | 60.81 | 6.43 | 1.68 | 28.01 | 24.92 | 25.52 | 25.72 |
| CW-500F | 60.22 | 6.65 | 1.50 | 29.59 | 24.70 | 25.37 | 25.60 |
| CW-750F | 75.64 | 5.89 | 4.08 | 9.91 | 31.44 | 33.57 | 31.91 |
| SFW-500P | 61.40 | 6.21 | 2.40 | 25.71 | 25.09 | 25.73 | 25.78 |
| SFW-750P | 56.27 | 6.16 | 2.37 | 32.70 | 22.51 | 23.11 | 23.14 |
| SFW-500F | 54.35 | 6.10 | 2.24 | 31.07 | 21.93 | 22.14 | 22.61 |
| SFW-750F | 78.20 | 5.12 | 6.91 | 6.53 | 31.94 | 34.15 | 31.83 |
| W-500P | 60.69 | 7.50 | 11.10 | 15.23 | 27.22 | 27.63 | 27.46 |
| W-750P | 58.07 | 7.16 | 11.85 | 15.69 | 25.97 | 25.97 | 26.01 |
| W-500F | 59.76 | 6.84 | 12.39 | 15.67 | 26.19 | 26.71 | 26.06 |
| W-750F | 69.74 | 5.69 | 11.90 | 8.41 | 29.32 | 30.87 | 28.87 |

[a] Dry basis.

### 3.3.4. Bio-char fraction

The final analysis and HHV of the various bio-char products produced during flash and conventional pyrolysis are both shown in Table 5**.** SFW contained more carbon than other materials, regardless of the pyrolysis technique. This element is crucial to determine the quality of a certain char as fuel. There was a tend characterised by an increase in the C content, within each type of pyrolysis once the temperature also raises. The highest values for this element were achieved, for the three materials, during conventional pyrolysis at 750 °C. When compared to CW and SFW, W had significantly less C and HHV data. For the case of hydrogen, the highest values were obtained for flash pyrolysis at a temperature of 500 °C. The high nitrogen values in wool are notorious (∼ 11 %). This fact was due to a large part of the nitrogen present in the original material remains after the pyrolytic process. These char N content may even be higher than the present in the original samples [80, 81]. Related to ash content, SFW had the lowest values (∼4 %). They were lower than the achieved by other authors for coals [82,83]. Pyrolysis temperatures of 750 °C increased the content of these undesirable materials in comparison to temperatures of 500 °C, with the exception of SFW-750P (which was also the sample with the lowest ash content, 3.58 %). Sulphur content (0.30–0.52 %) was low and similar for all the samples, being these results in line with the associated to other fuels chars derived from other biomass sources [84].

With reference to the HHV results, SFW was, again, the textile waste with better performance. For it, there was no clear difference neither for the type of pyrolysis used nor the temperature. With the exception of W-750F, where flash pyrolysis at 750 °C clearly had a negative impact on its HHV result (19.03 MJ/kg), this was maintained for the other bio-chars under study. This way, with values surrounding the 32 MJ/kg, the chars derived from SFW were, by far, the ones with a better energy power followed by CW (∼28.5 MJ/kg).

Bio-char from both flash and conventional pyrolysis was therefore suitable for use as fuel due to their high HHV and capacity to serve as adsorbent material precursors (from 56.95 % to 90.52 % of C content). Especially the use of SFW-750P was desirable. Textile waste characterisation values showed a better performance for pyrolytic behaviour when compared with other residues from similar nature studied in the literature [85].

## 3.4. Scanning electron microscope (SEM)

The study of the morphology and the elemental analysis of the surface of the textile residues (CW, SFW, W) as well as the different pyrolyzed samples was carried out by SEM-EDX. Fig. 7 shows some SEM images of the residues taken at different magnifications (500x and 2000x).

The image of the card waste (CW) shows a fibrous morphology along with irregular particles, which is consistent with its nature. This is a residue that is primarily made up of a mixture of seeds and cotton linters from the cotton screening process used in the carding work, Fig. 7. SFW shows a fully fibrous morphology due to its short-spun nature derived from rejection from batting, carding, and combing of cotton fibres, Fig. 7. The morphology of cotton fibres from CW and SFW residues, as specified in [86,87], is characterised by the torsion that the fibres present.

As for the wool residue (W), it presents a fibrous morphology characteristic of this type of material and, contrary to what happens with cotton fibres, there is no twist in the fibres, Fig. 7. The wool residue's fibres have a similar appearance to those described in some scientific publications [87,88], where the wool fibres are covered in tiny scales, a characteristic that the cotton fibres do not present. These outer woolly cuticle cells (or scales) overlap like tiles on a roof.

The CW sample EDX demonstrates the differences between the parts. The fibrous portion exhibits a surface and is primarily composed of C (50.6 %) and O (45.97 %), and some N (3.4 %), the CW non-fibrous part maintains high contents of C and O (41 %) with 5 % of N, 11.7 % of K and smaller proportion of S and Ca. The surface composition of SFW residue, short cotton fibre residue, preserves high contents of C and O (42.8 % and 51.9 % respectively), moderate K (4.6 %) and low N. As stated in [89], the EDX spectrum of untreated cotton fabric also shows high carbon (46.13 %) and oxygen (53.87 %) contents, which is consistent with our results.

Finally, in the W residue EDX spectrum of the wool residue, C (51.8 %) stands out as the main element, followed in importance by O (24.4 %), N (11.5 %) and S (7.08 %). Alkaline (K, Na) and alkaline earth (Ca) elements were also found, albeit in lower concentrations. In [88], goat wool, sheep wool and horse mane were studied by EDX and C, O, N and S stand out as major elements on the surface of the wool fibres and horsehair.

Fig. 8 shows some SEM images of the pyrolyzed residues under different conditions of the thermal process and taken at different magnifications (500x, 2000x and 10000x).

SEM images of CW-500F pyrolyzed material reveal that the fibrous nature of the parent material (CW) is preserved. The torsion of the cotton fibres, a typical feature of these materials, can be seen in detail in the image at a magnification of 10000 times. The cross section of a fibre bundle can be seen in the image at 2000x, Fig. 8. The higher temperature pyrolysis treatment seems to break the cotton fibres as can be seen in the 500x image of CW-750F where shorter fibres can be seen. In the same way, a generation of porosity is observed in the particles that accompany the fibres of this precursor, images at 2000x and 10000x of CW-750F. The pyrolyzed samples from the other cotton waste (SFW) also retain their fibrous morphology after the pyrolysis heat treatment, as can be seen in the 500x image of SFW-750P. Details of these fibres can be seen

**Table 5**
Chars ultimate analysis, HHV and ashes.

| | Ultimate analysis | | | | | HHV (MJ/kg) | Ash (%) |
|---|---|---|---|---|---|---|---|
| | C[a] (%) | H[a] (%) | N[a] (%) | S[a] (%) | O[ab] (%) | | |
| CW-500P | 77.99 ± 1.48 | 2.70 ± 0.14 | 1.11 ± 0.31 | 0.36 ± 0.01 | 8.54 | 28.96 | 9.29 |
| CW-750P | 82.29 ± 1.53 | 0.93 ± 0.07 | 1.19 ± 0.30 | 0.37 ± 0.00 | 5.48 | 28.43 | 9.74 |
| CW-500F | 75.42 ± 0.03 | 3.37 ± 0.11 | 1.11 ± 0.29 | 0.31 ± 0.06 | 10.39 | 28.71 | 9.41 |
| CW-750F | 80.87 ± 0.68 | 1.23 ± 0.14 | 1.05 ± 0.27 | 0.32 ± 0.06 | 6.71 | 28.15 | 9.82 |
| SFW-500P | 84.02 ± 1.71 | 2.92 ± 0.03 | 3.72 ± 0.40 | 0.47 ± 0.04 | 4.61 | 32.06 | 4.26 |
| SFW-750P | 90.52 ± 0.76 | 0.88 ± 0.11 | 3.70 ± 0.35 | 0.49 ± 0.01 | 0.83 | 32.01 | 3.58 |
| SFW-500F | 82.16 ± 0.66 | 3.41 ± 0.03 | 3.58 ± 0.26 | 0.49 ± 0.03 | 6.47 | 31.79 | 3.89 |
| SFW-750F | 87.03 ± 2.41 | 1.65 ± 0.35 | 3.04 ± 0.66 | 0.52 ± 0.04 | 3.21 | 31.50 | 4.56 |
| W-500P | 63.96 ± 1.36 | 2.28 ± 0.12 | 11.16 ± 0.88 | 0.33 ± 0.01 | 5.83 | 24.07 | 16.44 |
| W-750P | 69.20 ± 0.74 | 0.75 ± 0.02 | 9.66 ± 0.45 | 0.34 ± 0.01 | 1.37 | 24.45 | 18.68 |
| W-500F | 63.06 ± 0.98 | 3.15 ± 0.01 | 11.69 ± 0.76 | 0.30 ± 0.01 | 7.24 | 24.74 | 14.57 |
| W-750F | 56.95 ± 0.75 | 0.93 ± 0.12 | 8.88 ± 0.58 | 0.41 ± 0.04 | 9.71 | 19.03 | 23.12 |

[a] Dry basis.
[b] Determined by difference.

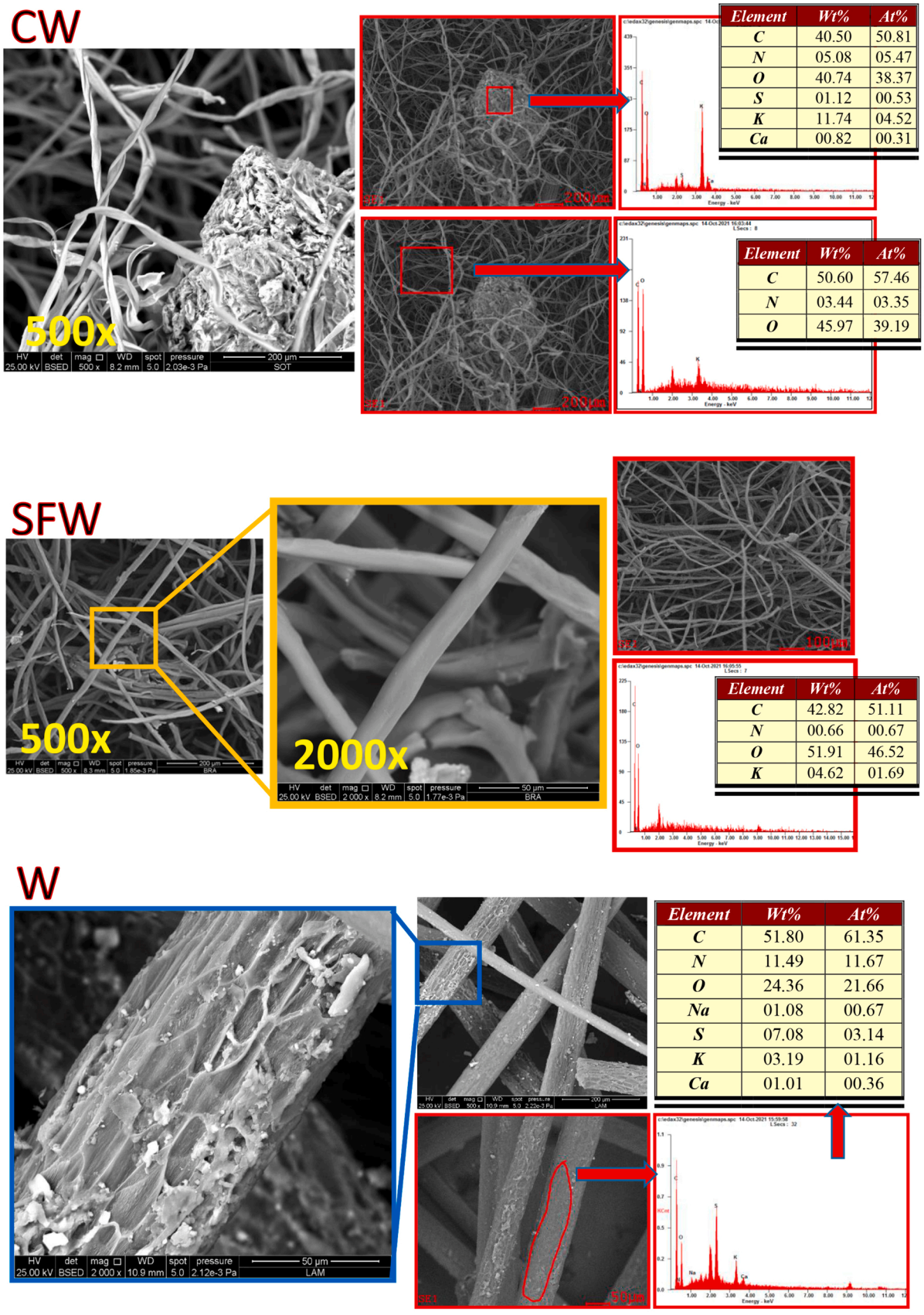


**Fig. 7.** Textile residues raw materials SEM-EDX.

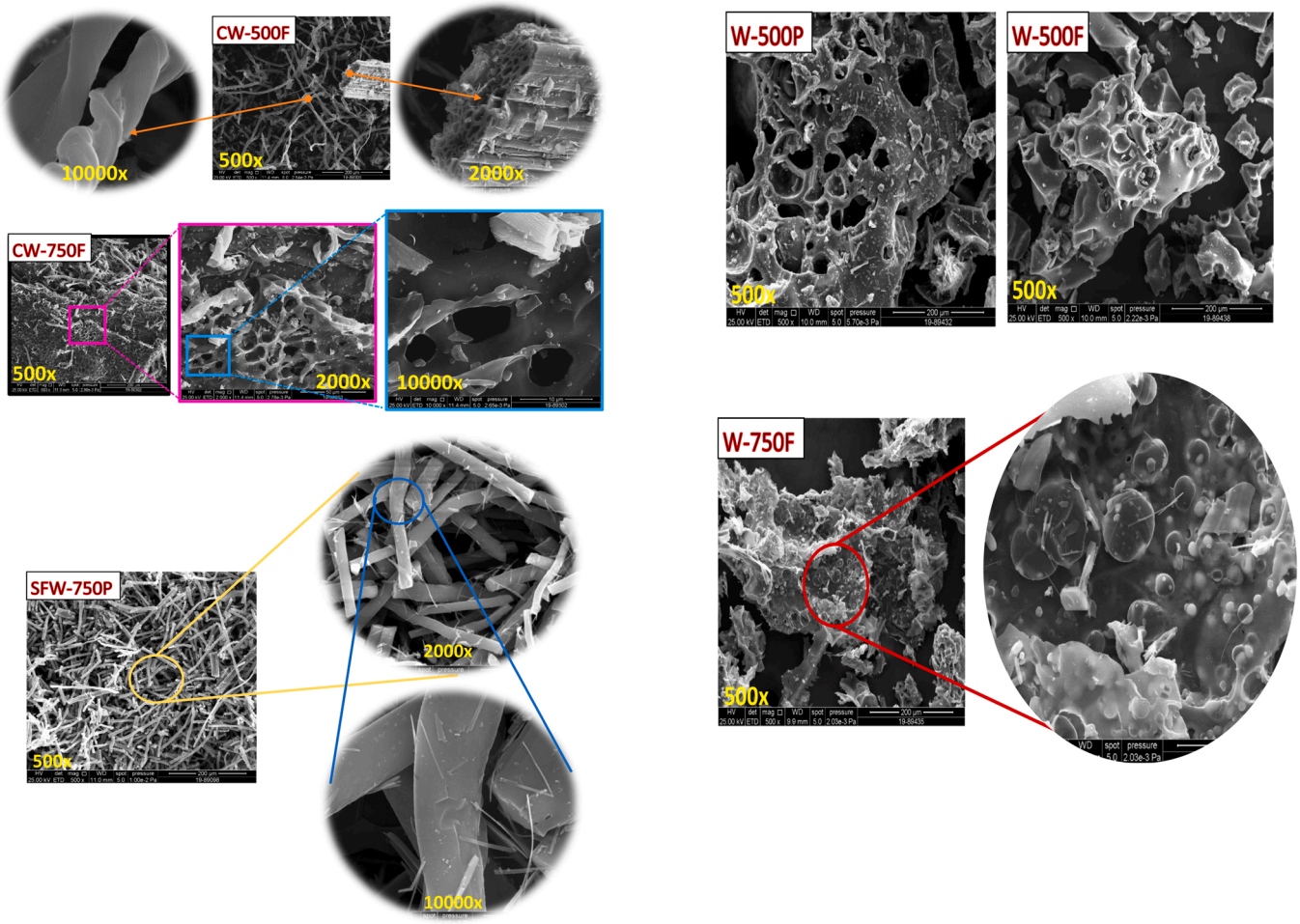


**Fig. 8.** Pyrolyzed waste SEM-EDX.

in the images that are at 2000x and 10000x.

Contrary to this behaviour, the pyrolyzed materials from the wool residual lose the precursor's fibrous shape regardless of the temperature heating process and the type of pyrolysis. Hence, particles of different sizes are obtained as can be seen in W-500P, W-500F and W-750F. These particles of the pyrolyzed samples present a large amount of porosity or holes through which the volatile matter has come out. The wool residue passed through a plastic phase during the pyrolysis process, forming vacuoles or devolatilization bubbles during the thermal process as a consequence of the release of volatile matter. Vacuoles or devolatilization bubbles can be seen in bio-char samples obtained with flash pyrolysis, being especially notable at high temperature, as can be seen in W-750F bio-char, Fig. 8.

## 4. Conclusions

An extensive experimental study on the conventional and flash pyrolysis has been performed on textile factory residues of animal (wool) and vegetable origin (card waste and short fibre waste) using an original pyrolysis oven. HHV and chemical characterisation of the samples revealed that they had good fuel properties. TGA analysis revealed differences between the DTG and TG profiles for the samples. CW and SFW released a greater amount of mass in a smaller temperature range compared to W. The highest DTG value was reached for SFW (16.937 %/min). Better results for all of the estimated thermal indices also supported the improved performance of SFW. Regarding fraction yield, the bio-oil fraction predominated for practically all the study conditions except for flash pyrolysis at 750 °C where gas is the majority fraction reaching values between 48 % and 56 %. SFW-500P denoted a bio-oil percentage of 55.12 %. Gas chromatographic analysis displayed a greater number of gaseous species in the case of flash pyrolysis. CO and $CO_2$ were the most emitted gases for CW and SFW, while in the pyrolysis of W, $O_2$ predominated. Oil fraction HHV results denoted a good thermal performance being the 750F the best pyrolysis conditions (34.15MJ/kg for SFW-750F). Contrary to high-temperature flash pyrolysis bio-oils, which are primarily made up of polycyclic aromatic hydrocarbons, conventional pyrolysis bio-oils and low temperature flash pyrolysis bio-oils both contain significant amounts of non-aromatic organic compounds. As chars is concerned, SFW was also the textile sample with better HHV and lower ash content (~32MJ/kg and ~4 % ash). SEM analysis revealed that, whereas for CW and SFW the torsion of the fibres was present, it was not so for W residue. This same analysis for the pyrolysis waste also denoted different behaviour with relation of the fibrous morphology.

## CRediT authorship contribution statement

**Begoña Ruiz:** Investigation, Data curation, Writing – original draft, Writing – review & editing, Methodology. **Enrique Fuente:** Conceptualization, Validation, Resources, Methodology, Investigation, Data curation. **Juan Marcos Sanz:** Investigation, Data curation, Resources. **Alejandro Pérez:** Investigation, Data curation, Methodology. **Luis Taboada-Ruiz:** Investigation, Data curation, Methodology. **L.F. Calvo:** Methodology, Validation, Investigation, Data curation, Writing – original draft. **Sergio Paniagua:** Investigation, Writing – review & editing, Visualization, Methodology.

## Declaration of Competing Interest

The authors declare that they have no known competing financial interests or personal relationships that could have appeared to influence the work reported in this paper.

## Data Availability

Data will be made available on request.

## Acknowledgements

Alejandro Pérez thanks to Spanish Research Council (CSIC) the JAE INTRO ICU SCHOLARSHIP 2019 [Ref. JAEICU-19-INCAR-15]. The authors thanks to the industry "Textil Santanderina, S.A." for providing the textile industrial wastes used in this research. In the same way, Sergio Paniagua thanks the Spanish research agency for the granting of the projects PDC2022-133394-I00 and PID2021-124347OB-I00, co-financed by the European Union.

## References

[1] S. Yousef, J. Eimontas, N. Striūgas, M. Tatariants, M.A. Abdelnaby, S. Tuckute, L. Kliucininkas, A sustainable bioenergy conversion strategy for textile waste with self-catalysts using mini-pyrolysis plant, Energy Convers. Manag. 196 (2019) 688–704, https://doi.org/10.1016/j.enconman.2019.06.050.

[2] P.E. Campbell, J.T. McMullan, B.C. Williams, F. Aumann, Co-combustion of coal and textiles in a small-scale circulating fluidised bed boiler in Germany, Fuel Process. Technol. 67 (2000) 115–129, https://doi.org/10.1016/S0378-3820(00)00094-1.

[3] N. Nørup, K. Pihl, A. Damgaard, C. Scheutz, Development and testing of a sorting and quality assessment method for textile waste, Waste Manag. 79 (2018) 8–21, https://doi.org/10.1016/J.WASMAN.2018.07.008.

[4] H. Zhao, B. Lin, Will agglomeration improve the energy efficiency in China's textile industry: Evidence and policy implications, Appl. Energy 237 (2019) 326–337, https://doi.org/10.1016/J.APENERGY.2018.12.068.

[5] Recycling in textile and waste disposal | Interreg Europe, (n.d.). https://www.interregeurope.eu/reset/events/event/322/recycling-in-textile-and-waste-disposal/ (Accessed September 21, 2021).

[6] B.K. Ozsel, Valorization of textile waste hydrolysate for hydrogen gas and levulinic acid production, Int. J. Hydrogen Energy 46 (2021) 4992–4997, https://doi.org/10.1016/j.ijhydene.2020.11.080.

[7] Y.P. Rago, D. Surroop, R. Mohee, Torrefaction of textile waste for production of energy-dense biochar using mass loss as a synthetic indicator, J. Environ. Chem. Eng. 6 (2018) 811–822, https://doi.org/10.1016/j.jece.2017.12.055.

[8] Y. Hu, C. Du, N. Pensupa, C.S.K. Lin, Optimisation of fungal cellulase production from textile waste using experimental design, Process Saf. Environ. Prot. 118 (2018) 133–142, https://doi.org/10.1016/j.psep.2018.06.009.

[9] D. Xu, Y. Zhang, B. Chen, J. Bai, G. Liu, B. Zhang, Identifying the critical paths and sectors for carbon transfers driven by global consumption in 2015, Appl. Energy 306 (2022), 118137, https://doi.org/10.1016/J.APENERGY.2021.118137.

[10] X. Zhuang, H. Zhan, Y. Huang, Y. Song, X. Yin, C. Wu, Conversion of industrial biowastes to clean solid fuels via hydrothermal carbonization (HTC): upgrading mechanism in relation to coalification process and combustion behavior, Bioresour. Technol. 267 (2018) 17–29, https://doi.org/10.1016/j.biortech.2018.07.002.

[11] C. Ryu, A.N. Phan, V.N. Sharifi, J. Swithenbank, Co-combustion of textile residues with cardboard and waste wood in a packed bed, Exp. Therm. Fluid Sci. 32 (2007) 450–458, https://doi.org/10.1016/J.EXPTHERMFLUSCI.2007.05.008.

[12] L.J.R. Nunes, R. Godina, J.C.O. Matias, J.P.S. Catalão, Economic and environmental benefits of using textile waste for the production of thermal energy, J. Clean. Prod. 171 (2018) 1353–1360, https://doi.org/10.1016/j.jclepro.2017.10.154.

[13] Y. Du, T. Ju, Y. Meng, T. Lan, S. Han, J. Jiang, A review on municipal solid waste pyrolysis of different composition for gas production, Fuel Process. Technol. 224 (2021), 107026, https://doi.org/10.1016/J.FUPROC.2021.107026.

[14] Z. Xu, R. Qi, M. Xiong, D. Zhang, H. Gu, W. Chen, Conversion of cotton textile waste to clean solid fuel via surfactant-assisted hydrothermal carbonization: mechanisms and combustion behaviors, Bioresour. Technol. 321 (2021), 124450, https://doi.org/10.1016/j.biortech.2020.124450.

[15] J. González-Arias, X. Gómez, M. González-Castaño, M.E. Sánchez, J.G. Rosas, J. Cara-Jiménez, Insights into the product quality and energy requirements for solid biofuel production: a comparison of hydrothermal carbonization, pyrolysis and torrefaction of olive tree pruning, Energy 238 (2022), 122022, https://doi.org/10.1016/J.ENERGY.2021.122022.

[16] X. Sun, Z. Zhu, F. Zaman, Y. Huang, Y. Guan, Detection and kinetic simulation of animal hair/wool wastes pyrolysis toward high-efficiency and sustainable management, Waste Manag. 131 (2021) 305–312, https://doi.org/10.1016/J.WASMAN.2021.06.018.

[17] J.O. Ighalo, F.U. Iwuchukwu, O.E. Eyankware, K.O. Iwuozor, K. Olotu, O.C. Bright, C.A. Igwegbe, Flash pyrolysis of biomass: a review of recent advances, Clean. Technol. Environ. Policy 24 (8) (2022) 2349–2363, https://doi.org/10.1007/S10098-022-02339-5.

[18] H. Yuan, H. Fan, R. Shan, M. He, J. Gu, Y. Chen, Study of synergistic effects during co-pyrolysis of cellulose and high-density polyethylene at various ratios, Energy Convers. Manag 157 (2018) 517–526.

[19] K. Salmeia, M. Jovic, A. Ragaisiene, Z. Rukuiziene, R. Milasius, D. Mikucioniene, S. Gaan, Flammability of cellulose-based fibers and the effect of structure of phosphorus compounds on their flame retardancy, Polymers 8 (2016) 293, https://doi.org/10.3390/polym8080293.

[20] D. Chen, K. Cen, X. Zhuang, Z. Gan, J. Zhou, Y. Zhang, H. Zhang, Insight into biomass pyrolysis mechanism based on cellulose, hemicellulose, and lignin: evolution of volatiles and kinetics, elucidation of reaction pathways, and characterization of gas, biochar and bio-oil, Combust. Flame 242 (2022), 112142, https://doi.org/10.1016/J.COMBUSTFLAME.2022.112142.

[21] D. Fiaschi, G. Manfrida, L. Russo, L. Talluri, Improvement of waste heat recuperation on an industrial textile dryer: Redesign of heat exchangers network and components, Energy Convers. Manag. 150 (2017) 924–940, https://doi.org/10.1016/J.ENCONMAN.2017.05.053.

[22] P.L. Dulong, A.T. Petit. Recherches sur la mesure des temperatures et sur les lois de la communication de la chaleur, 1st ed..,, De l'Imprimerie royale,, Paris, 1818.

[23] Beckman David, Techno-economic assessment of selected biomass liquefaction processes, Valt. Tek. Tutk., Espoo; Hels. (1990).

[24] A. Friedl, E. Padouvas, H. Rotter, K. Varmuza, Prediction of heating values of biomass fuel from elemental composition, Anal. Chim. Acta 544 (2005) 191–198.

[25] L. Fagbemi, L. Khezami, R. Capart, Pyrolysis products from different biomasses: application to the thermal cracking of tar, Appl. Energy 69 (2001) 293–306.

[26] X. Li, B. Ma, L. Xu, Z. Hu, X. Wang, Thermogravimetric analysis of the co-combustion of the blends with high ash coal and waste tyres, Thermochim. Acta 441 (2006) 79–83, https://doi.org/10.1016/J.TCA.2005.11.044.

[27] T.L. Jiang, W.S. Chen, M.J. Tsai, H.H. Chiu, A numerical investigation of multiple flame configurations in convective droplet gasification, Combust. Flame 103 (1995) 221–238, https://doi.org/10.1016/0010-2180(95)92244-2.

[28] S.-W. Du, W.-H. Chen, J.A. Lucas, Pulverized coal burnout in blast furnace simulated by a drop tube furnace, Energy 35 (2010) 576–581, https://doi.org/10.1016/J.ENERGY.2009.10.028.

[29] S. Paniagua, L. Escudero, R.N. Coimbra, C. Escapa, M. Otero, L.F. Calvo, Effect of applying organic amendments on the pyrolytic behavior of a poplar energy crop, Waste Biomass Valoriz. 9 (2018) 1435–1449, https://doi.org/10.1007/s12649-017-9885-1.

[30] S.L. Niu, C.M. Lu, K.H. Han, J.L. Zhao, Thermogravimetric analysis of combustion characteristics and kinetic parameters of pulverized coals in oxy-fuel atmosphere, J. Therm. Anal. Calor. 98 (2009) 267, https://doi.org/10.1007/s10973-009-0133-1.

[31] S. Fang, Z. Yu, Y. Lin, Y. Lin, Y. Fan, Y. Liao, X. Ma, Effects of additives on the co-pyrolysis of municipal solid waste and paper sludge by using thermogravimetric analysis, Bioresour. Technol. 209 (2016) 265–272, https://doi.org/10.1016/J.BIORTECH.2016.03.027.

[32] Z.Y. Gao, L.J. Fang, J. Zhou, W.P. Yan, Research on the combustion performance of blended coal in thermal-balance, Power Eng. 22 (2002) 1764–1767.

[33] S. Fang, Z. Yu, Y. Lin, S. Hu, Y. Liao, X. Ma, Thermogravimetric analysis of the co-pyrolysis of paper sludge and municipal solid waste, Energy Convers. Manag. 101 (2015) 626–631, https://doi.org/10.1016/J.ENCONMAN.2015.06.026.

[34] Y. Lin, Y. Liao, Z. Yu, S. Fang, Y. Lin, Y. Fan, X. Peng, X. Ma, Co-pyrolysis kinetics of sewage sludge and oil shale thermal decomposition using TGA–FTIR analysis, Energy Convers. Manag. 118 (2016) 345–352, https://doi.org/10.1016/J.ENCONMAN.2016.04.004.

[35] W. Saadi, S. Rodríguez-Sánchez, B. Ruiz, S. Souissi-Najar, A. Ouederni, E. Fuente, Pyrolysis technologies for pomegranate (Punica granatum L.) peel wastes. Prospects in the bioenergy sector, Renew, Energy 136 (2019) 373–382, https://doi.org/10.1016/j.renene.2019.01.017.

[36] A. Pérez, B. Ruiz, E. Fuente, L.F. Calvo, S. Paniagua, Pyrolysis technology for Cortaderia selloana invasive species. Prospects in the biomass energy sector, Renew. Energy 169 (2021) 178–190, https://doi.org/10.1016/J.RENENE.2021.01.015.

[37] A. Ahmed, M.S. Abu Bakar, R.S. Sukri, M. Hussain, A. Farooq, S. Moogi, Y.K. Park, Sawdust pyrolysis from the furniture industry in an auger pyrolysis reactor system for biochar and bio-oil production, Energy Convers. Manag. 226 (2020), 113502, https://doi.org/10.1016/J.ENCONMAN.2020.113502.

[38] P. Halder, S. Kundu, S. Patel, R. Parthasarathy, B. Pramanik, J. Paz-Ferreiro, K. Shah, TGA-FTIR study on the slow pyrolysis of lignin and cellulose-rich fractions derived from imidazolium-based ionic liquid pre-treatment of sugarcane straw, Energy Convers. Manag. 200 (2019), 112067, https://doi.org/10.1016/J.ENCONMAN.2019.112067.

[39] B. Biswas, N. Pandey, Y. Bisht, R. Singh, J. Kumar, T. Bhaskar, Pyrolysis of agricultural biomass residues: Comparative study of corn cob, wheat straw, rice straw and rice husk, Bioresour. Technol. 237 (2017) 57–63, https://doi.org/10.1016/j.biortech.2017.02.046.

[40] L. Reyes, L. Abdelouahed, C. Mohabeer, J.C. Buvat, B. Taouk, Energetic and exergetic study of the pyrolysis of lignocellulosic biomasses, cellulose, hemicellulose and lignin, Energy Convers. Manag. 244 (2021), 114459, https://doi.org/10.1016/J.ENCONMAN.2021.114459.

[41] N.A. Nudri, W.A. Wan Abdul Karim Ghani, R. Thomas Bachmann, B.T.H. T. Baharudin, D.K.S. Ng, M.S.Md Said, Co-combustion of oil palm trunk biocoal/

sub-bituminous coal fuel blends, Energy Convers. Manag.: X 10 (2021), 100072, https://doi.org/10.1016/J.ECMX.2020.100072.
[42] J. He, L. Li, H. Feng, M. Jiang, J. Li, L. Guo, J. Zhang, P. Zhang, J. Gong, Q. Huang, Morphology and nanostructure of flame-formed soot particles from combustion of typical municipal solid waste, Fuel Process. Technol. 232 (2022), 107269, https://doi.org/10.1016/J.FUPROC.2022.107269.
[43] S. Aramkitphotha, H. Tanatavikorn, C. Yenyuak, T. Vitidsant, Low sulfur fuel oil from blends of microalgae pyrolysis oil and used lubricating oil: Properties and economic evaluation, Sustain. Energy Technol. Assess. 31 (2019) 339–346, https://doi.org/10.1016/J.SETA.2018.12.019.
[44] Z.R. Gajera, K. Verma, S.P. Tekade, A.N. Sawarkar, Kinetics of co-gasification of rice husk biomass and high sulphur petroleum coke with oxygen as gasifying medium via TGA, Bioresour. Technol. Rep. 11 (2020), 100479, https://doi.org/10.1016/J.BITEB.2020.100479.
[45] S. Paniagua, M. Otero, R.N.R. Coimbra, C. Escapa, A.A.I. García, L.F.L. Calvo, Simultaneous thermogravimetric and mass spectrometric monitoring of the pyrolysis, gasification and combustion of rice straw, J. Therm. Anal. Calor. 121 (2015) 603–611, https://doi.org/10.1007/s10973-015-4632-y.
[46] B. Fekhar, V. Zsinka, N. Miskolczi, Value added hydrocarbons obtained by pyrolysis of contaminated waste plastics in horizontal tubular reactor: In situ upgrading of the products by chlorine capture, J. Clean. Prod. 241 (2019), 118166, https://doi.org/10.1016/J.JCLEPRO.2019.118166.
[47] G.S. Nyashina, G.V. Kuznetsov, P.A. Strizhak, Effects of plant additives on the concentration of sulfur and nitrogen oxides in the combustion products of coal-water slurries containing petrochemicals, Environ. Pollut. 258 (2020), 113682, https://doi.org/10.1016/J.ENVPOL.2019.113682.
[48] S. Das, Physical and chemical properties of wool, sheep wool and mutton, Prod. Value Addit. (2021) 97.
[49] A. Hegyi, C. Dico, H. Szilagyi, Sheep wool thermal insulating mattresses behaviour in the water vapours presence, Procedia Manuf. 46 (2020) 410–417, https://doi.org/10.1016/J.PROMFG.2020.03.060.
[50] R. Zhao, L. Liu, Y. Bi, L. Tian, X. Wang, Determination of pyrolysis characteristics and thermo-kinetics to assess the bioenergy potential of Phragmites communis, Energy Convers. Manag. 207 (2020), 112510, https://doi.org/10.1016/J.ENCONMAN.2020.112510.
[51] S. Gaur, T.B. Reed, Thermal Data for Natural and Synthetic Fuels, Marcel Deeker, in: Inc.: New York, NY, USA, 1998: pp. 239–241.
[52] V. Dhyani, T. Bhaskar, A comprehensive review on the pyrolysis of lignocellulosic biomass, Renew. Energy 129 (2018) 695–716, https://doi.org/10.1016/j.renene.2017.04.035.
[53] L.S. Thakur, A.K. Varma, P. Mondal, Analysis of thermal behavior and pyrolytic characteristics of vetiver grass after phytoremediation through thermogravimetric analysis, J. Therm. Anal. Calorim. 131 (3) (2017) 3053–3064, https://doi.org/10.1007/S10973-017-6788-0.
[54] C. He, C. Tang, W. Liu, L. Dai, R. Qiu, Co-pyrolysis of sewage sludge and hydrochar with coals: pyrolytic behaviors and kinetics analysis using TG-FTIR and a discrete distributed activation energy model, Energy Convers. Manag. 203 (2020), 112226, https://doi.org/10.1016/J.ENCONMAN.2019.112226.
[55] S. Barisci, M. Öncel, The disposal of combed cotton wastes by pyrolysis, Int J. Green. Energy 11 (2014), https://doi.org/10.1080/15435075.2013.772516.
[56] H. Liu, J. Zhang, J. Liu, L. Chen, H. Huang, F. Evrendilek, Co-pyrolytic mechanisms and products of textile dyeing sludge and durian shell in changing operational conditions, Chem. Eng. J. 420 (2021), 129711, https://doi.org/10.1016/J.CEJ.2021.129711.
[57] Y. Wu, C. Wen, X. Chen, G. Jiang, G. Liu, D. Liu, Catalytic pyrolysis and gasification of waste textile under carbon dioxide atmosphere with composite Zn-Fe catalyst, Fuel Process. Technol. 166 (2017) 115–123, https://doi.org/10.1016/J.FUPROC.2017.05.025.
[58] R. Miranda, C. Sosa-Blanco, D. Bustos-Martínez, C. Vasile, Pyrolysis of textile wastes: I. Kinetics and yields, J. Anal. Appl. Pyrolysis 80 (2007) 489–495, https://doi.org/10.1016/J.JAAP.2007.03.008.
[59] A. Pulyalina, I. Faykov, V. Nesterova, M. Goikhman, I. Podeshvo, N. Loretsyan, A. Novikov, I. Gofman, A. Toikka, G. Polotskaya, Novel polyester amide membranes containing biquinoline units and complex with cu(i): synthesis, characterization, and approbation for n-heptane isolation from organic mixtures, Polymers 12 (2020) 645, https://doi.org/10.3390/POLYM12030645.
[60] P. Zhu, S. Sui, B. Wang, K. Sun, G. Sun, A study of pyrolysis and pyrolysis products of flame-retardant cotton fabrics by DSC, TGA, and PY–GC–MS, J. Anal. Appl. Pyrolysis 71 (2004) 645–655, https://doi.org/10.1016/J.JAAP.2003.09.005.
[61] C. Zhou, Y. Zhang, Y. Liu, Z. Deng, X. Li, L. Wang, J. Dai, Y. Song, Z. Jiang, J. Qu, A. A. Siyal, Co-pyrolysis of textile dyeing sludge and red wood waste in a continuously operated auger reactor under microwave irradiation, Energy 218 (2021), 119398, https://doi.org/10.1016/J.ENERGY.2020.119398.
[62] X. Peng, X. Ma, Y. Lin, Z. Guo, S. Hu, X. Ning, Y. Cao, Y. Zhang, Co-pyrolysis between microalgae and textile dyeing sludge by TG–FTIR: Kinetics and products, Energy Convers. Manag. 100 (2015) 391–402, https://doi.org/10.1016/J.ENCONMAN.2015.05.025.
[63] G.K. Parshetti, A. Quek, R. Betha, R. Balasubramanian, TGA–FTIR investigation of co-combustion characteristics of blends of hydrothermally carbonized oil palm biomass (EFB) and coal, Fuel Process. Technol. 118 (2014) 228–234, https://doi.org/10.1016/J.FUPROC.2013.09.010.
[64] S. Paniagua, L. Zanfaño, L.F. Calvo, Influence of the fertilizer type in the agronomic and energetic behaviour of the residues coming from oleander, cypress and quinoa, Fuel 272 (2020), 117711, https://doi.org/10.1016/J.FUEL.2020.117711.
[65] S.Al Arni, Comparison of slow and fast pyrolysis for converting biomass into fuel, Renew. Energy 124 (2018) 197–201, https://doi.org/10.1016/J.RENENE.2017.04.060.
[66] B. Babinszki, Z. Sebestyén, E. Jakab, L. Kőhalmi, J. Bozi, G. Várhegyi, L. Wang, Skreiberg, Z. Czégény, Effect of slow pyrolysis conditions on biocarbon yield and properties: characterization of the volatiles, Bioresour. Technol. 338 (2021), 125567, https://doi.org/10.1016/J.BIORTECH.2021.125567.
[67] A. Oasmaa, Y. Solantausta, V. Arpiainen, E. Kuoppala, K. Sipila, Fast pyrolysis bio-oils from wood and agricultural residues, Energy Fuels 24 (2010) 1380–1388.
[68] D. Czajczyńska, L. Anguilano, H. Ghazal, R. Krzyżyńska, A.J. Reynolds, N. Spencer, H. Jouhara, Potential of pyrolysis processes in the waste management sector, Therm. Sci. Eng. Prog. 3 (2017) 171–197, https://doi.org/10.1016/J.TSEP.2017.06.003.
[69] C. Balcik-Canbolat, B. Ozbey, N. Dizge, B. Keskinler, Pyrolysis of commingled waste textile fibers in a batch reactor: Analysis of the pyrolysis gases and solid product, Int. J. Green Energy 14 (2017) 289–294.
[70] D. Kwon, S. Yi, S. Jung, E.E. Kwon, Valorization of synthetic textile waste using $CO_2$ as a raw material in the catalytic pyrolysis process, Environ. Pollut. 268 (2021), 115916, https://doi.org/10.1016/J.ENVPOL.2020.115916.
[71] R. Abdallah, A. Juaidi, M. Assad, T. Salameh, F. Manzano-Agugliaro, Energy recovery from waste tires using pyrolysis: palestine as case of study, Energies 13 (2020) 1817, https://doi.org/10.3390/EN13071817.
[72] K. Maliutina, A. Tahmasebi, J. Yu, S.N. Saltykov, Comparative study on flash pyrolysis characteristics of microalgal and lignocellulosic biomass in entrained-flow reactor, Energy Convers. Manag. 151 (2017) 426–438, https://doi.org/10.1016/j.enconman.2017.09.013.
[73] N. Zhou, J. Zhou, L. Dai, F. Guo, Y. Wang, H. Li, W. Deng, H. Lei, P. Chen, Y. Liu, Syngas production from biomass pyrolysis in a continuous microwave assisted pyrolysis system, Bioresour. Technol. 314 (2020), 123756.
[74] F. Yaşar, Comparision of fuel properties of biodiesel fuels produced from different oils to determine the most suitable feedstock type, Fuel 264 (2020), 116817, https://doi.org/10.1016/J.FUEL.2019.116817.
[75] A. Farooq, H.W. Lee, J. Jae, E.E. Kwon, Y.-K. Park, Emulsification characteristics of ether extracted pyrolysis-oil in diesel using various combinations of emulsifiers (Span 80, Atlox 4916 and Zephrym PD3315) in double reactor system, Environ. Res. 184 (2020), 109267.
[76] S. Bilgen, S. Keleş, K. Kaygusuz, Calculation of higher and lower heating values and chemical exergy values of liquid products obtained from pyrolysis of hazelnut cupulae, Energy 41 (2012) 380–385.
[77] O. Konur, Biomass pyrolysis and pyrolysis oils: a review of the research, Biodiesel Fuels (2021) 153–169.
[78] M. Anwar, M.G. Rasul, N. Ashwath, The efficacy of multiple-criteria design matrix for biodiesel feedstock selection, Energy Convers. Manag 198 (2019), 111790.
[79] Phenanthrene | 85-01-8, (n.d.). https://www.chemicalbook.com/ChemicalProductProperty_EN_CB8854465 (Accessed December 27, 2022).
[80] L.I. Darvell, C. Brindley, X.C. Baxter, J.M. Jones, A. Williams, Nitrogen in biomass char and its fate during combustion: a model compound approach, Energy Fuels 26 (2012) 6482–6491, https://doi.org/10.1021/EF201676T.
[81] Z. Gong, Z. Wang, Z. Wang, P. Fang, F. Meng, Study on pyrolysis characteristics of tank oil sludge and pyrolysis char combustion, Chem. Eng. Res. Des. 135 (2018) 30–36, https://doi.org/10.1016/J.CHERD.2018.05.027.
[82] J. Zhu, L. Jin, Y. Luo, H. Hu, Y. Xiong, B. Wei, D. Wang, Fast co-pyrolysis of a massive Naomaohu coal and cedar mixture using rapid infrared heating, Energy Convers. Manag. 205 (2020), 112442, https://doi.org/10.1016/J.ENCONMAN.2019.112442.
[83] H. Zhao, Q. Song, S. Liu, Y. Li, X. Wang, X. Shu, Study on catalytic co-pyrolysis of physical mixture/staged pyrolysis characteristics of lignite and straw over an catalytic beds of char and its mechanism, Energy Convers. Manag. 161 (2018) 13–26, https://doi.org/10.1016/J.ENCONMAN.2018.01.083.
[84] D. Pradhan, R.K. Singh, H. Bendu, R. Mund, Pyrolysis of Mahua seed (Madhuca indica) – Production of biofuel and its characterization, Energy Convers. Manag. 108 (2016) 529–538, https://doi.org/10.1016/J.ENCONMAN.2015.11.042.
[85] R.B. Silva, S. Martins-Dias, C. Arnal, M.U. Alzueta, M. Costa, Pyrolysis and char characterization of refuse-derived fuel components, Energy Fuels 29 (2015) 1997–2005, https://doi.org/10.1021/EF502011F.
[86] K. Kafle, K. Greeson, C. Lee, S.H. Kim, Cellulose polymorphs and physical properties of cotton fabrics processed with commercial textile mills for mercerization and liquid ammonia treatments*:, Https://Doi.Org/10.1177/0040517514527379. 84, 2014, pp. 1692–1699. https://doi.org/10.1177/0040517514527379.
[87] M. del Egido, T. Calderón, La ciencia y el arte: ciencias experimentales y conservación del Patrimonio Histórico, Madrid (2008).
[88] A. Ahmed, A. Qayoum, F.Q. Mir, Spectroscopic studies of renewable insulation materials for energy saving in building sector, J. Build. Eng. 44 (2021), https://doi.org/10.1016/J.JOBE.2021.103300.
[89] N.A. Ibrahim, B.M. Eid, E.A. El-Aziz, T.M. Abou Elmaaty, S.M. Ramadan, Multifunctional cellulose-containing fabrics using modified finishing formulations, RSC Adv. 7 (2017) 33219–33230, https://doi.org/10.1039/C7RA05403C.